

The Derivation and Quasinormal Mode Spectrum of Acoustic Anti-de Sitter Black  
Hole Analogues

by

James Patrick Babb  
B.Sc., University of Winnipeg, 2010

A Thesis Submitted in Partial Fulfillment of the  
Requirements for the Degree of

MASTER OF SCIENCE

in the Department of Physics and Astronomy

© James Babb, 2013  
University of Victoria

All rights reserved. This thesis may not be reproduced in whole or in part, by  
photocopying or other means, without the permission of the author.

The Derivation and Quasinormal Mode Spectrum of Acoustic Anti-de Sitter Black  
Hole Analogues

by

James Patrick Babb  
B.Sc., University of Winnipeg, 2010

Supervisory Committee

---

Dr. Pavel Kovtun, Supervisor  
(Department of Physics and Astronomy)

---

Dr. Adam Ritz, Departmental Member  
(Department of Physics and Astronomy)

---

Dr. Florin Diacu, Outside Member  
(Department of Mathematics and Statistics)

## Supervisory Committee

---

Dr. Pavel Kovtun, Supervisor  
(Department of Physics and Astronomy)

---

Dr. Adam Ritz, Departmental Member  
(Department of Physics and Astronomy)

---

Dr. Florin Diacu, Outside Member  
(Department of Mathematics and Statistics)

---

## ABSTRACT

Dumb holes (also known as acoustic black holes) are fluid flows which include an “acoustic horizon:” a surface, analogous to a gravitational horizon, beyond which sound may pass but never classically return. Soundwaves in these flows will therefore experience “effective geometries” which are identical to black hole spacetimes up to a conformal factor. By adjusting the parameters of the fluid flow, it is possible to create an effective geometry which is conformal to the Anti-de Sitter black hole spacetime—a geometry which has received a great deal of attention in recent years due to its conjectured holographic duality to Conformal Field Theories. While we would not expect an acoustic analogue of the AdS-CFT correspondence to exist, this dumb hole provides a means, at least in principle, of experimentally testing the theoretical properties of the AdS spacetime. In particular, I have calculated the quasinormal mode spectrum of this acoustic geometry.

# Contents

<b>Supervisory Committee</b>	<b>ii</b>
<b>Abstract</b>	<b>iii</b>
<b>Table of Contents</b>	<b>iv</b>
<b>List of Tables</b>	<b>vi</b>
<b>List of Figures</b>	<b>vii</b>
<b>Acknowledgements</b>	<b>ix</b>
<b>Dedication</b>	<b>x</b>
<b>1 Introduction</b>	<b>1</b>
<b>2 Theoretical Background</b>	<b>4</b>
2.1 What is a Quasinormal Mode? . . . . .	4
2.1.1 Types of Quasinormal Mode . . . . .	4
2.1.2 Applying Boundary Conditions . . . . .	5
2.2 Anti-de Sitter Spacetime and the AdS-CFT Correspondence . . . . .	6
2.2.1 AdS-CFT Correspondence . . . . .	8
2.2.2 Discussion . . . . .	12
2.3 Acoustic Black Holes . . . . .	12
2.3.1 Derivation . . . . .	13
2.3.2 Acoustic Horizons . . . . .	15
2.3.3 Acoustic Hawking Radiation . . . . .	16
2.4 Experimental Realization . . . . .	17
<b>3 Derivation of the Acoustic AdS Black Hole</b>	<b>20</b>

3.1	Selecting the Proper Form of the Metric . . . . .	20
3.2	Deriving the fluid parameters . . . . .	23
3.2.1	Constraints from Fluid Mechanics . . . . .	24
3.3	Coordinate Transformation Between Metrics . . . . .	26
<b>4</b>	<b>Quasinormal Modes of Acoustic Black Holes</b>	<b>31</b>
4.1	Quasinormal Modes of Acoustic Geometries Conformal to Asymptotically-Anti de Sitter Black Holes . . . . .	32
4.2	Quasinormal Modes of Acoustic Geometries Conformal to Asymptotically Flat Black Holes . . . . .	40
<b>5</b>	<b>Conclusions</b>	<b>48</b>
	<b>Bibliography</b>	<b>50</b>
<b>A</b>	<b>Derivation of Painlevé -Gullstrand-like coordinates</b>	<b>53</b>
<b>B</b>	<b>Derivation of the Coordinate transformation between representations of Anti-de Sitter Black Hole Geometry</b>	<b>55</b>

# List of Tables

Table 4.1	Real and imaginary components of the frequency eigenvalues, $\omega M$ , for scalar perturbations of the AdS Schwarzschild conformal dumb hole, for various values of the angular quantum number with $\frac{M}{L} = 10$ . . . . .	39
Table 4.2	Real and imaginary frequency eigenvalues, $\omega 2M$ for scalar perturbations of the flat-space Schwarzschild-conformal dumb hole, for various values of the angular quantum number. . . . .	45

# List of Figures

Figure 2.1	A simple example of a negative curvature space in two dimensions.	6
Figure 2.2	Black hole temperature as a function of horizon radius. For values small compared to the curvature of the universe, AdS black holes are, like their flat-space counterparts, thermodynamically unstable. However, when their radius is large in comparison to the curvature of the spacetime, they obtain a positive specific heat capacity, and so become thermodynamically stable. . . . .	7
Figure 2.3	$N_c$ D-branes in flat space. Image taken from “String Theory and Quantum Chromodynamics,” David Mateos, 2007 [1] . . . . .	9
Figure 2.4	Geometry in the presence of a stack of D-branes. At low coupling, the radius $R$ approaches zero, and the D-branes may thus be regarded as infinitely-thin spacetime defects. Image taken from “String Theory and Quantum Chromodynamics,” David Mateos, 2007 [1] . . . . .	10
Figure 2.5	A stack of d-branes at low energy at weak (left) and strong (right) coupling. What if the physics they describe are the same? (based upon diagrams taken from “String Theory and Quantum Chromodynamics,” David Mateos, 2007) [1] . . . . .	11
Figure 2.6	The potential experienced by the atoms of the Bose-Einstein condensate at some time before the minimum of the harmonic potential (a) is moved over to the step potential (b). The dashed line in the harmonic potential corresponds to the chemical potential of the BEC. Gravity points in the $-x$ direction. Image taken from “Realization of a sonic black hole analogue in a Bose-Einstein condensate,” Oren Lahav et al, 2009 [2] . . . . .	17

- Figure 2.7 The Bose-Einstein condensate before (a) and after (b) crossing over the step potential. The dashed yellow line represents the approximate location of the acoustic horizon, while the dotted-dashed yellow line represents the position where the flow slows to a subsonic velocity. Image taken from “Realization of a sonic black hole analogue in a Bose-Einstein condensate,” Oren Lahav et al, 2009 . . . . . 19
- Figure 4.1 The behaviour of the real part of a simple plane wave for increasing values of  $t$ . The red (medium-shade) curve represents both ingoing and outgoing solutions (with  $C_- = C_+ = 1$ ) at  $t = 0$ . As time increases, we see that our  $C_+ e^{+ik(u - \frac{\omega}{k}t)}$  term (in green/lightest shade) moves to the left, whereas our  $C_- e^{-ik(u - \frac{\omega}{k}t)}$  (in blue/darkest shade) moves to the right. . . . . 36
- Figure 4.2 The behaviour of the real parts of our quasinormal mode solutions for increasing values of  $t$ . The red (medium-shade) curve represents both ingoing and outgoing solutions (with  $C_- = C_+ = 1$ ) at  $t = 0$ . As time increases, we see that our  $C_-$  term (in green/lightest shade) moves towards the horizon, whereas our  $C_+$  term (in blue/darkest shade) moves away from it. . . . . 37
- Figure 4.3 The QNM frequencies,  $M\omega$  plotted in the complex plane for various values of  $l$ , with  $\frac{M}{L} = 10$ . Red (solid circular) points correspond to  $l = 0$ , orange (square) to  $l = 1$ , yellow (diamond) to  $l = 2$ , green (upward-facing triangle) to  $l = 3$ , blue (downward-facing triangle) to  $l = 4$  and violet (hollow circle) to  $l = 5$ . The frequency scales in units of  $\text{length}^{-1}$ . . . . . 38
- Figure 4.4 Possible spectrum of quasinormal frequencies for the Flat-Space Schwarzschild-conformal dumb hole, at varying values of the angular momentum quantum number  $l$ , with  $2M = 1$ . Red (solid circle) corresponds to  $l = 0$ , orange (square) to  $l = 1$ , yellow (diamond) to  $l = 2$  and green (upward-facing triangle) to  $l = 3$ . The frequency scales in units of  $\text{length}^{-1}$ . . . . . 46

## ACKNOWLEDGEMENTS

This thesis would not have been possible without a great deal of support from other people. In no particular order, I would like to thank:

**my friend and occasional girlfriend, Leah Jane Grantham** for suffering through my endless parade of personal crises,

**the other Physics graduate students at the University of Victoria** for empathizing with my struggles in the way that only other graduate students can,

**my family** if it wasn't for our regular conversations, I would sincerely doubt my capacity to remain sane,

**Dr. Gabor Kunstatter, Dr. Dwight Vincent and Dr. Murray Alexander** , all of Winnipeg, Manitoba, for their interest and occasional input into my thesis project, and for providing me with a welcome opportunity to speak on the subject

**the programming teams** behind the diffgeo.m package for Mathematica and the grtensor package for Maple, without whom this research could literally not have been undertaken, and last but not least,

**Dr. Pavel Kovtun** for his input, suggestions, and near-infinite patience.

*“You just keep on trying till you run out of cake.”*

GlaDOS, *Portal*, 2007

## DEDICATION

This thesis is respectfully dedicated to Mr. Dilyn J. M. Wilkinson and Ms. Vallery Lancey, both of Victoria, British Columbia, for demonstrating to me that my life can be my own if I but choose to make it so.

# Chapter 1

## Introduction

Black holes have been, without doubt, one of the most interesting concepts to emerge from Einstein's theory of general relativity. While the idea of a region of spacetime so severely warped that not even light can ever (classically) escape from it has a way of seizing the imagination all by itself, black holes have attracted even more attention since it became apparent that they also exemplified certain quantum mechanical properties. The early 1970s witnessed a key result in this direction: Stephen Hawking's celebrated derivation of black hole radiance [3] [4], accomplished without the benefit of a theory of quantum gravity. Ever since then, black holes have often been used as theoretical "laboratories" for testing-out the interactions between quantum theory and gravity. This process has only accelerated since Maldacena's postulation of the Anti-de Sitter - Conformal Field Theory (AdS-CFT) correspondence [5]. This correspondence implies that quantum field theories in  $n$  flat dimensions can be described in terms of gravity in  $n + 1$  dimensional Anti-de Sitter spacetimes.

There is, however, a seemingly insurmountable problem when it comes to all predictions of black hole behaviour, no matter how theoretically rigorous: namely, they are very difficult to test experimentally. We cannot create black holes in the lab, and all of those naturally-occurring ones which have been detected astronomically are so far from Earth as to be almost impossible to observe in detail, rendering observations of subtle, quantum mechanical properties such as Hawking radiation all but impossible. In the case of black holes in Anti-de Sitter spacetimes, this problem is further compounded by the fact that such geometries do not even appear to be relevant for cosmology or astrophysics.

Acoustic black holes (also known as "dumb holes") may provide a partial way around this problem. First postulated by Bill Unruh in 1981 [6], these are supersonic

fluid flows through which sound propagates in a manner analogous to that of light in a black hole geometry; that is to say that there exists a threshold in the flow at which the fluid velocity exceeds the speed of sound in the fluid, and from beyond which no sound waves can ever (classically) escape. In analogy with the *event* horizon of a gravitational black hole, this threshold is known as an *acoustic* horizon.

This sonic geometry effectively reproduces the “kinematic” properties of a black hole [7] (i.e, those properties which depend only upon the geometry of spacetime): in particular, since it can be shown that Hawking radiation is not a gravitational property at all (but in fact depends only upon the existence of a horizon and the presence of quantized background fields), we should expect a dumb hole to emit a thermal gas of phonons (provided that it exists in a medium, such as a superfluid, in which sound is quantized). Likewise, we can usefully ask how perturbations of a scalar field propagate through this geometry. Note, however, that the dumb hole’s dynamics are in fact governed by the fluid equations of motion (rather than by Einstein’s equations, as in a gravitational black hole), and so we should not expect any phenomena analogous to black hole properties which use Einstein’s equations in their derivations. Thus, it is not useful to talk about the gravitational perturbations of the effective spacetime.

Over the years, a number of different acoustic black hole “spacetimes” have been derived (for an extensive review of examples, please see [8] ), and indeed, some have been created experimentally [2] (although Hawking radiation and scalar perturbations have yet to be observed). In this thesis, I will be deriving a dumb hole geometry that is conformal to the Anti-de Sitter (AdS) black hole in four dimensions (the first such dumb hole to be derived). I will then compute the scalar quasinormal modes for this particular geometry. These are the perturbations of the scalar field which die off in time, in the manner of the ringing of a bell; mathematically, they are the formal solutions of a linear differential equation which have complex frequency eigenvalues. For a review of quasinormal modes, please see [9].

My interest in the Anti-de Sitter black hole geometry is motivated by its theoretical significance in the AdS-CFT correspondence. According to this hypothesis, quasinormal mode frequencies in the AdS spacetime are associated with the poles of the correlation functions of the dual field theory [10]. While it would be tempting to think that an acoustic AdS geometry might also come with its own analogous corresponding field theory, the fact that acoustic geometries do not arise from gravity appears (as will be seen) to preclude this idea. Nevertheless such acoustic geometries

could prove useful in that they could allow researchers, at least in principle, to experimentally (albeit qualitatively) test the validity of theoretical predictions made on the gravitational side of the correspondence.

Formally, my thesis will be structured as follows:

Chapter 2 will be an overview of the theoretical background of this problem, broken down into three broad streams. I shall first discuss the concept of quasinormal modes: what they are and what boundary conditions they accept in the case of black hole geometries. I shall then discuss the properties of AdS black hole spacetimes in general, paying especial attention to the apparent change of stability which takes place as a black hole goes from being larger than the universe’s radius of curvature to being smaller than it. I shall also provide a broad overview of the AdS-CFT correspondence, showing how it supposedly arises from string theoretical considerations as well as discussing the interpretation of quasinormal modes in this hypothesis. This will also give me a chance to explain why we should not expect an analogue of the AdS-CFT duality to emerge from acoustic fluid flows. Finally, I will walk-through the derivation of acoustic black holes following the work of Bill Unruh and Matt Visser, showing how “acoustic geometries” emerge naturally from the linearized versions of the fluid equations of motion.

In chapter 3, I shall derive an acoustic analogue of the four-dimensional AdS black hole by demanding a metric of a particular form satisfy the Einstein equations for the geometry. By comparing this metric to the general acoustic metric, I will be able to identify the behaviour that is required of the fluid’s pressure, density and velocity profile. I shall also derive the conformal factor between the acoustic metric and the gravitational metric, and work-out the unit transformation necessary to go between the derived representation of the space-time and its typical, static form.

Chapter 4 will consist of the actual calculation of the quasinormal frequencies of the acoustic AdS black hole analogue using the Frobenius method. I will then calculate the complex frequency eigenvalues by applying appropriate boundary conditions, and summarize my results in a table. I shall also, incidentally, calculate the (possible) quasinormal frequencies of an acoustic flat-space black hole analogue, using Leaver’s Hill determinant method [11].

Finally, in chapter 5, I will discuss the theoretical significance of my findings.

# Chapter 2

## Theoretical Background

The aim of this thesis (as has been noted in the previous chapter) is to calculate the scalar quasinormal mode spectrum of an Anti-de Sitter dumb hole. This naturally brings up three questions:

- 1) What is a quasinormal mode?
- 2) What is the Anti-de Sitter spacetime (and why is it interesting)?, and
- 3) What is a dumb hole?

In this chapter, each of these questions will be answered in sequence.

### 2.1 What is a Quasinormal Mode?

A quasinormal mode is a perturbation of a field which decays in time. A simple example of this would come from tapping a bell or wine glass, causing it to ring with a linear combination of its natural frequencies; if this ringing carried-on forever, it would be “normal;” however, it does not; it is damped (mathematically, its frequency has an imaginary component) and so it dies down over time.

For our purposes, quasinormal modes are formal solutions of linear differential equations (in particular, the Klein-Gordon equation for our effective metric), having time-dependence  $e^{-i\omega t}$ , which have complex frequency eigenvalues. For reviews of QNMs, please see [9], [12],[13].

#### 2.1.1 Types of Quasinormal Mode

The type of quasinormal mode will depend upon which ordinary differential equation we are perturbing. For example, the equation for a massless scalar field in curved

spacetime will be given by:

$$\frac{1}{\sqrt{-g}} \frac{\partial}{\partial x^\mu} (\sqrt{-g} g^{\mu\nu} \frac{\partial}{\partial x^\mu} \psi) = 0. \quad (2.1)$$

The equation for the scalar quasinormal modes can therefore be found simply by taking the perturbative expansion about some known solution  $\psi_0: \psi = \psi_0 + \epsilon \psi_1$ , to linear order. Likewise, we can consider the electromagnetic quasinormal modes by considering Maxwell's equations in curved spacetimes:

$$\partial_\mu (\sqrt{-g} g^{\mu\nu} g^{\sigma\rho} F_{\nu\rho}) = 0, \quad (2.2)$$

where  $F_{\nu\rho}$  is the electromagnetic tensor  $\partial_\nu A_\rho - \partial_\rho A_\nu$ . Here we are taking perturbations of the vector potential  $A_\mu = A_\mu^0 + \epsilon A_\mu^1$ . We may also consider linearized perturbations of the Einstein equations,

$$G_{\mu\nu} + g_{\mu\nu} \Lambda = 0, \quad (2.3)$$

where we are taking perturbations about some background metric,  $g_{\mu\nu} = g_{\mu\nu}^0 + \epsilon h_{\mu\nu}$ . In this case note that the Einstein Tensor,  $G_{\mu\nu}$  itself depends on the metric, so for a particular background (and corresponding values of the Ricci scalar and cosmological constant), we will, in the case of gravitational quasinormal modes, have to derive a set of ‘‘linearized Einstein equations.’’

### 2.1.2 Applying Boundary Conditions

While a variety of methods exist to solve these equations, it is only through the application of boundary conditions to the solutions that we can work out the spectrum of quasinormal frequencies. In flat space, the boundary conditions are defined to be ingoing at the horizon, and outgoing at spatial infinity [9]. However, we will be looking at an effective spacetime that is conformal to that of the AdS black hole; in such a spacetime (for reasons that are to be discussed in the following section), it does not make sense to speak of modes being outgoing at spatial infinity. Rather, we will be applying the condition that the modes die-off at spatial infinity [14]: this is known as the ‘‘Dirichlet’’ boundary condition.

## 2.2 Anti-de Sitter Spacetime and the AdS-CFT Correspondence

Anti-de Sitter spacetimes are ones which possess a constant, negative scalar curvature; that is to say that they are Lorentzian analogues of hyperbolic space (as the Minkowski metric is a Lorentzian analogue of Euclidean space). Physically, this means that every given point in such a spacetime is a saddle point, and the overall curvature is like that of a trumpet bell (rather than the surface of a sphere—an instance of positive curvature). For an overview of AdS Spacetimes, see for example, [15], section 4.7.

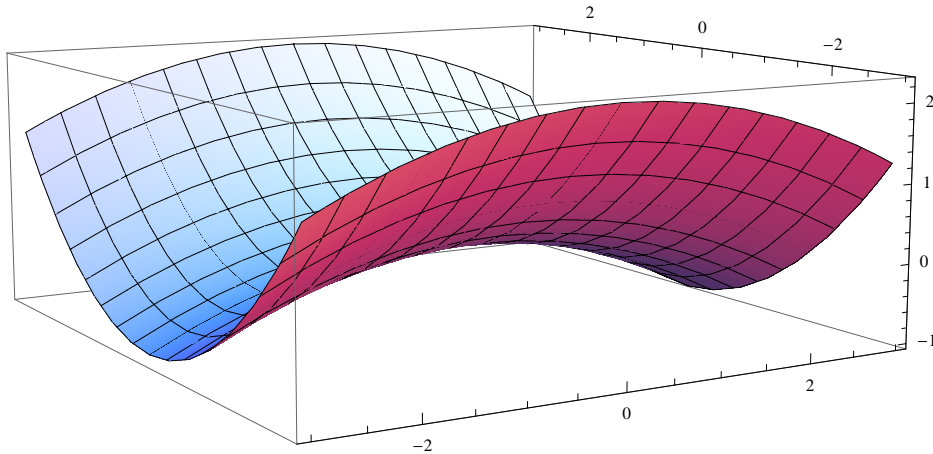


Figure 2.1: A simple example of a negative curvature space in two dimensions.

In Einstein's general relativity, however, note that geometric curvature corresponds to gravitational force. In this case (since the curvature is negative) this will be an *attractive* force, resulting in a gravitational potential which increases with distance from any origin. As such, it is not possible for any massive particle to escape to infinity. Massless particles, by contrast, *can* escape, but they will be infinitely redshifted [16].

The line element for such a spacetime, in three plus one dimensions, is given by:

$$ds^2 = -V dt^2 + V^{-1} dr^2 + r^2(d\theta^2 + \sin^2(\theta)d\phi^2), \quad (2.4)$$

with  $V = 1 + \frac{r^2}{L^2}$ , and  $L = \left(-\frac{3}{\Lambda}\right)^{1/2}$  (with  $\Lambda$  being the cosmological constant). Note that all expressions in this section are rendered in natural units (i.e,  $c = G = \hbar = k_b = 1$ ).

We may embed a Schwarzschild black hole in this spacetime by redefining  $V$  as

$$V = 1 + \frac{r^2}{L^2} - \frac{2m}{r} \quad (2.5)$$

(with  $m$  the mass of the black hole).

Black holes in this spacetime have unusual thermodynamic properties [16]. In particular, it can be shown that the black hole's temperature,  $T$ , is given by:

$$T_{bh} = \frac{L^2 + 3r_0^2}{4\pi L^2 r_0}, \quad (2.6)$$

where  $r_0$  is the black hole's horizon radius,

$$r_0 = \frac{1}{3}(27mL^2 + 3\sqrt{3L^6 + 81m^2L^4})^{1/3} - \frac{L^2}{(27mL^2 + 3\sqrt{3L^6 + 81m^2L^4})^{1/3}}. \quad (2.7)$$

The temperature achieves a minimum value of  $T = \frac{\sqrt{3}}{2\pi L}$  at the point  $r_0 = \frac{L}{\sqrt{3}}$ , going to infinity as  $r_0$  gets both shorter and longer.

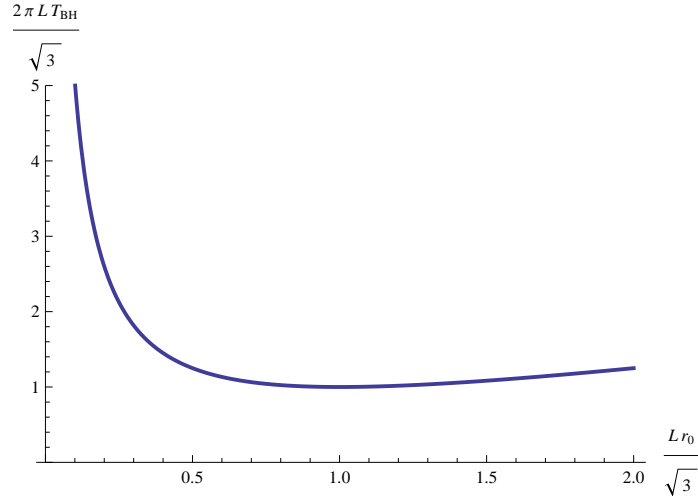


Figure 2.2: Black hole temperature as a function of horizon radius. For values small compared to the curvature of the universe, AdS black holes are, like their flat-space counterparts, thermodynamically unstable. However, when their radius is large in comparison to the curvature of the spacetime, they obtain a positive specific heat capacity, and so become thermodynamically stable.

Physically, this is due to the fact that, when the horizon is small compared to the radius of curvature ( $\sim \frac{1}{L}$ ) the black hole simply behaves like one in flat space. That

is to say, it has a temperature that is inversely proportional to its horizon radius. On the other hand, when a black hole has a radius big enough to detect the curvature, it's temperature starts to increase with increasing radius.

Looking at our expression for horizon radius, we can see that it increases with increasing values of mass (which is, of course, interchangeable with energy). Thus, we find that for black holes of a radius of less than  $r_0 = \frac{L}{\sqrt{3}}$ , temperature actually *decreases* as a function of the amount of energy added to the system; that is to say, small black holes have negative specific heat capacities and are therefore thermodynamically unstable. Large black holes, by contrast, have positive specific heat capacities; their temperature *increases* with added energy, and so they are thermodynamically stable (see figure 2.2).

### 2.2.1 AdS-CFT Correspondence

The AdS-CFT correspondence is a hypothetical duality between a gauge theory in  $n$ -dimensional Minkowski spacetime and gravity in an  $n + 1$  dimensional Anti-de Sitter universe which arises from type II (b) string theory[17]. In particular, the correspondence justifies a longstanding expectation of theoretical physics that a gauge theory with a large number of colours should be related to string theory [18], and systematizes this duality by identifying parameters in the two theories with one another (see [19] for a review). Much of the interest in this theory is motivated by the fact that it is, in general, far easier to work out results using the bulk gravitational theory than it is to work out such results using the gauge theory on the boundary. As such, there is some hope that the duality may be able to help describe Quantum Chromodynamics, at least in a qualitative way.

For some very brief background, string theory is an attempt to unify gravity with the other forces of nature by postulating that rather than being infinitesimal points, elementary degrees of freedom (including both massive particles and force carriers) are in fact made-out of “strings,” with finite lengths  $l_s$  (on the order of the Planck scale), oscillating in ten dimensions. These strings are parameterized by their lengths, their tension, and their coupling constant  $g_s$ . Different excitations of these strings correspond to different elementary particles. They may be either open or closed, but if they are open, then their open ends must be connected to a “Dirichlet p-brane” (otherwise known as a Dp-brane, or simply D-Brane: an extended object in  $p$  spatial dimensions defined as a boundary condition for open strings). The version

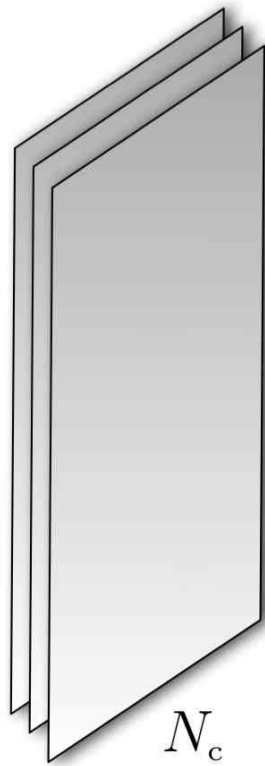


Figure 2.3:  $N_c$  D-branes in flat space. Image taken from “String Theory and Quantum Chromodynamics,” David Mateos, 2007 [1]

of the theory that includes super-symmetric particles is known as superstring theory [20][21].

With this out of the way, let us now consider (in the context of type II b string theory) the case of a stack of  $N_c$  separate D3-branes situated in a flat ten-dimensional spacetime, with ten dimensions being the number being predicted by superstring theory (for accessible descriptions of the situation, see [1] and [21], chapter 23). The string theory has both open and closed string degrees of freedom. Since D3-branes are massive objects, they alter the geometry of the spacetime around them.

In particular, in the immediate vicinity of the branes, spacetime is warped into a “throat” geometry in the form of a five-dimensional AdS spacetime, with the remaining five dimensions being “compactified:” that is to say, rolled-up into the finite-sized sphere  $S_5$ . Asymptotically, of course, the spacetime retains its original ten-dimensional Minkowski form.

This throat has a particular radius  $R$ , given by the formula:

$$R^4 = 4\pi g_s N_c l_s^4. \quad (2.8)$$

For fixed values of the number of branes  $N_c$  and the string length  $l_s$ , it follows

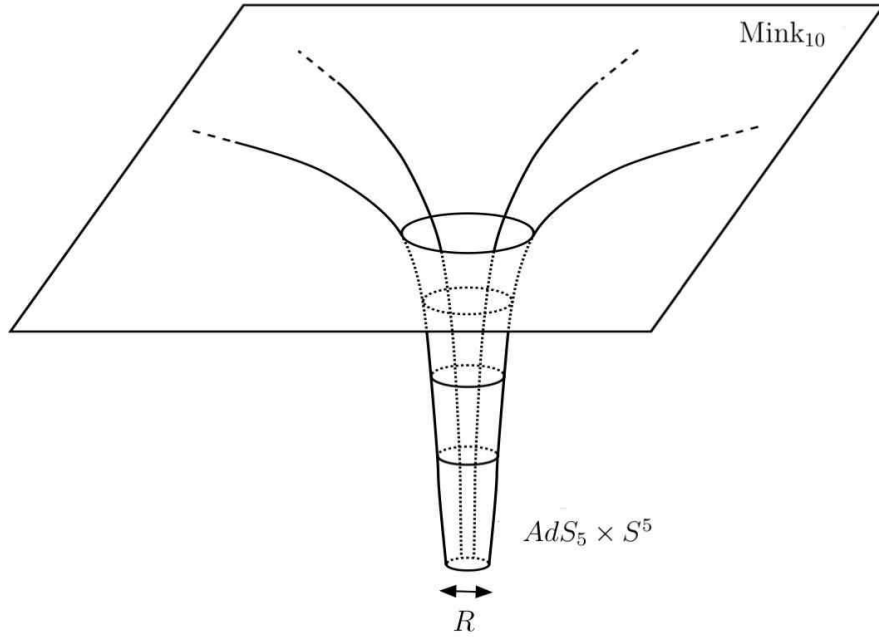


Figure 2.4: Geometry in the presence of a stack of D-branes. At low coupling, the radius  $R$  approaches zero, and the D-branes may thus be regarded as infinitely-thin spacetime defects. Image taken from “String Theory and Quantum Chromodynamics,” David Mateos, 2007 [1]

that this radius should go to zero as the coupling,  $g_s$ , becomes small (i.e.  $g_s \ll 1$ ). In this case, the throat essentially closes-up, and so the D3 brane stack can thus be thought of as an infinitely thin defect in 10-dimensional Minkowski spacetime, to which open strings are attached. Note, however, that in the opposite limit (that is to say,  $g_s \gg 1$ ), the radius becomes very large in comparison to the string length  $l_s$  and so we can think of the closed strings as propagating through an  $AdS_5 \times S^5$  geometry. The branes, for their part, disappear behind a horizon at the infinite “end” of the throat, and along with them, so do the open-string modes.

We may now consider the low-energy limits of the two extremes. The interactions involving closed strings (both with each other and with open strings) are governed by the coupling constant  $GE$ , where  $G$  is Newton’s gravitational constant and  $E$  is the energy. Thus, when  $E$  is very low, the closed string modes decouple, and we are left, in the  $g_s \ll 1$  limit, with a bunch of open strings propagating through the 3+1 dimensional worldvolume of the Branes. This, as it turns out, describes a QCD-like theory, only with  $N_c$  colours (rather than 3).

In the opposite ( $g_s N_c \gg 1$ ) limit, we find that at low energy, closed strings in the throat are incapable of escaping to the asymptotic Minkowski space. Thus, the throat modes decouple from the flat space modes, and we are left with a theory of closed strings in an  $AdS_5 \times S^5$  spacetime: a gravitational theory.

It is important to note that the underlying physics between the two regimes has not changed: if we were to ‘dial-up’ the coupling constant from the low-energy case,

we would go from having open strings in 3+1 dimensional flat space to having closed strings in 4+1 dimensional Anti-de Sitter space. Hence, we obtain the AdS-CFT correspondence.

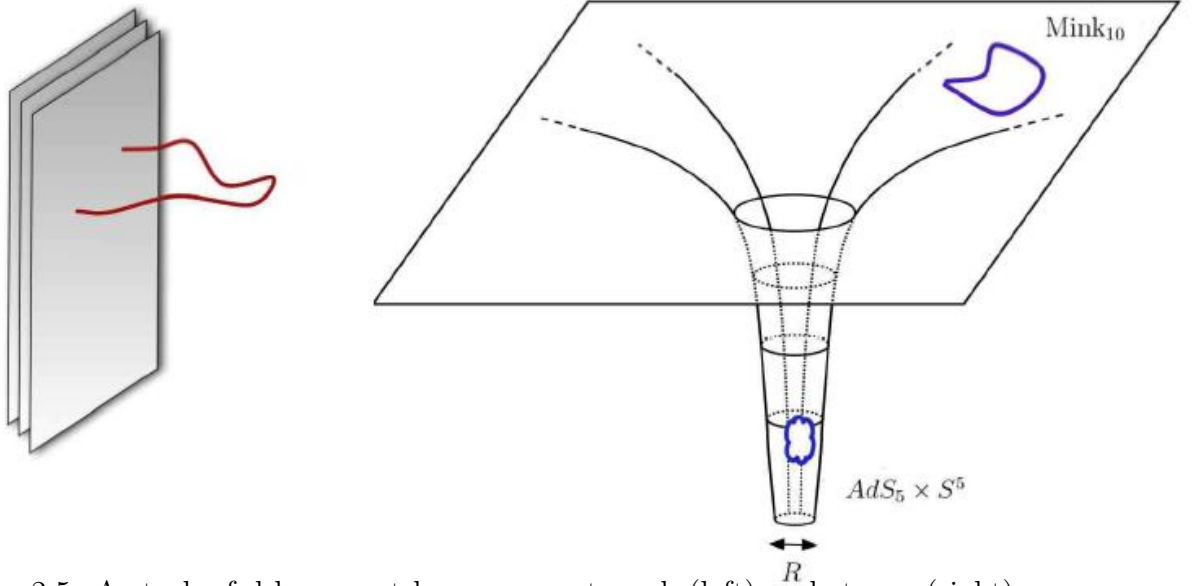


Figure 2.5: A stack of d-branes at low energy at weak (left) and strong (right) coupling. What if the physics they describe are the same? (based upon diagrams taken from “String Theory and Quantum Chromodynamics,” David Mateos, 2007) [1]

In particular, it is possible, through consideration of the various symmetries on both sides of the duality, to identify the string theory parameters (at small coupling) with the field theory parameters (at large coupling) [19]. This allows us to make identifications between *fields* in the  $N$  dimensional (“bulk”) gravitational theory, and *operators* in  $N - 1$  dimensional (“boundary”) field theory. Theoretical physicists may find this identification useful, as it is, in general, much easier to perform calculations in General Relativity than it is to do so in a strongly-coupled gauge theory.

We can relate this to our above discussion of quasinormal modes [10] [22]. Let us consider the behaviour of a field,  $Z$ , in an AdS-black hole spacetime; in the vicinity of the horizon, we will have a purely ingoing solution which is a linear combination of the possible solutions ( $\phi_1$  and  $\phi_2$ ) at the boundary:

$$Z(r) = A\phi_1(r) + B\phi_2(r). \quad (2.9)$$

The coefficients in this expression will generally depend upon the parameters of the differential equation, such as momentum and frequency. Near the boundary, this solution becomes

$$Z(r) = Ar^{-\Delta_-}(1 + \dots) + Br^{-\Delta_+}(1 + \dots), \quad (2.10)$$

where  $\Delta_-$  and  $\Delta_+$  are the lower and higher exponents of the differential equation at the boundary (and ellipses denote higher powers of “ $1/r$ ”). It turns out that the retarded correlation function of two operators in the dual field theory will be given by [10]

$$\langle OO \rangle_R \propto \frac{B}{A} + \text{Contact terms}. \quad (2.11)$$

By solving for the Dirichlet boundary conditions of the quasinormal modes, we are in fact finding the frequencies at which  $A$  goes to 0. Thus, quasinormal frequencies correspond to the poles of the correlation functions in the dual theory.

### 2.2.2 Discussion

One thing that is important to note about the above explanation is that the correspondence between the bulk and the boundary is strictly due to the underlying physics of the situation. That is to say that this duality with field theory in  $n - 1$  dimensions is a property of the *supergravity* in an AdS spacetime- it is *not* a property of the Anti-de Sitter geometry itself. Thus, if we could see such a geometry arise in a non-gravitational manner (for a suggestive example, as the “acoustic geometry” of a particular fluid flow), there would be no reason to expect any duality to field theory. However, such a geometry could, at least potentially, allow for experimental tests of the theoretically-predicted geometric properties of AdS spacetimes.

## 2.3 Acoustic Black Holes

In general, predictions made by black hole physics are very difficult to test experimentally, for the very simple reason that naturally-occurring black holes are not conveniently located for direct observation, and the prospects of creating one in the lab seem extraordinarily remote. However, certain properties of black holes may be observable through the creation of analogous entities. More particularly, it is possible to create “effective geometries” for soundwaves by manipulating the flow of the fluid through which they are propagating [6]; at places where the speed of the fluid’s flow exceeds the speed of sound in that fluid, we will see the formation of “acoustic

horizons.” Just as spacetime geometry ensures that (classically) no electromagnetic radiation may ever leave, so too does fluid geometry prevent any soundwaves from ever propagating outwards. However, since Hawking radiation is a property of the horizon itself (whether or not it actually emerges from gravitational considerations) [3] [7], it can be shown that, in media in which soundwaves are quantized, acoustic horizons should emit a thermal radiation of phonons.

### 2.3.1 Derivation

Let us consider a non-relativistic, irrotational fluid which is also “barotropic” (i.e, its pressure depends only upon its density) and non-viscous [6] [23]; it is thus described by three equations. The continuity equation [24]:

$$\frac{\partial \rho}{\partial t} + \vec{\nabla} \cdot (\rho \vec{v}) = 0, \quad (2.12)$$

The (non-viscous) Euler equation [24]

$$\rho \left( \frac{\partial \vec{v}}{\partial t} + (\vec{v} \cdot \vec{\nabla}) \vec{v} \right) = -\vec{\nabla} p, \quad (2.13)$$

and a barotropic equation of state

$$p = p(\rho), \quad (2.14)$$

where  $\vec{v}$  is fluid velocity,  $p$  is pressure,  $t$  is time and  $\rho$  is mass-density.

We demand an irrotational fluid for the purpose of simplicity; it is much easier for us to think of velocity as being the gradient of a scalar field,  $\vec{v} = \vec{\nabla} \Psi$ , which necessarily implies that the vorticity,  $\vec{\omega} = \vec{\nabla} \times \vec{v} = 0$ ; this has the effect of causing sound (which, as we will see, is just a perturbation of velocity) to *also* be describable in terms of a scalar field. Demanding a barotropic fluid further simplifies the situation by ensuring that vorticity remains zero at all times; this can easily be demonstrated by taking the curl of the Euler equation, which will yield the time evolution of vorticity. This time derivative will go to zero if the initial value of vorticity is zero and pressure depends exclusively upon density. The zero-viscosity constraint, meanwhile, is in place because viscosity would break the Acoustic Lorentz Invariance).

Suppose that we have an exact solution to equations (2.12), (2.13) and (2.14), given by  $[\rho_0(t, \vec{x}), p_0(t, \vec{x}), \Psi_0(t, \vec{x})]$ . Now let us consider linear fluctuations around

this background:

$$\rho(t, \vec{x}) = \rho_0(t, \vec{x}) + \epsilon \rho_1(t, \vec{x}) + \dots \quad (2.15)$$

$$p(t, \vec{x}) = p_0(t, \vec{x}) + \epsilon p_1(t, \vec{x}) + \dots \quad (2.16)$$

$$\Psi(t, \vec{x}) = \Psi_0(t, \vec{x}) + \epsilon \Psi_1(t, \vec{x}) + \dots \quad (2.17)$$

Substituting the perturbed solutions into equations (2.13) and (2.14), as well as Taylor-expanding equation (2.15) about  $\rho_0$ , it can be shown that we obtain:

$$\frac{\partial \rho_1}{\partial t} + \vec{\nabla} \cdot (\rho_1 \vec{\nabla} \Psi_0 + \rho_0 \vec{\nabla} \Psi_1) = 0, \quad (2.18)$$

$$\rho_0 \left( \frac{\partial \Psi_1}{\partial t} + \vec{\nabla} \Psi_0 \cdot \vec{\nabla} \Psi_1 \right) = p_1 \text{ and} \quad (2.19)$$

$$p_1 = \left( \frac{\partial p}{\partial \rho} \right) \rho_1, \quad (2.20)$$

where  $\frac{\partial p}{\partial \rho} = c_s^2$ ,  $c_s$  being the speed of sound in the fluid. These can be combined into the second-order partial differential equation:

$$\frac{\partial}{\partial t} \left( c_s^{-2} \rho_0 \left( \frac{\partial \Psi_1}{\partial t} + \vec{v}_0 \cdot \vec{\nabla} \Psi_1 \right) \right) = \vec{\nabla} \cdot \left( \rho_0 \vec{\nabla} \Psi_1 - c_s^{-2} \rho_0 \vec{v}_0 \left( \frac{\partial \Psi_1}{\partial t} + \vec{v}_0 \cdot \vec{\nabla} \Psi_1 \right) \right), \quad (2.21)$$

where  $\vec{v}_0 = \vec{\nabla} \Psi_0$  is the background velocity profile. Note that for a static background (with  $p_0$  and  $\rho_0$  equal to constants, and  $\vec{v}_0 = 0$ , this reduces to the equation:

$$\frac{1}{c_s^2} \frac{\partial^2 \psi_1}{\partial t^2} = \vec{\nabla}^2 \psi_1, \quad (2.22)$$

which describes the propagation of waves through a fluid medium travelling at the speed of sound. We therefore conclude that the function  $\psi_1$  describes sound waves.

By introducing the four-by-four matrix

$$g^{\mu\nu}(t, \vec{x}) \equiv \frac{1}{\rho_0 c_s} \begin{pmatrix} -1 & \vdots & -v_0^j \\ \cdots & \cdot & \cdots \\ -v_0^i & \vdots & (c_s^2 \delta^{ij} - v_0^i v_0^j) \end{pmatrix}, \quad (2.23)$$

equation (2.21) may be written as:

$$\frac{1}{\sqrt{-g}} \frac{\partial}{\partial x^\mu} (\sqrt{-g} g^{\mu\nu} \frac{\partial}{\partial x^\mu} \Psi_1) = 0 \quad (2.24)$$

(where  $x^\mu$  is the four vector  $(t, x, y, z)$  and we are using Einstein's summation notation) and  $g$  is the inverse determinant of the matrix). This equation is, of course, formally identical to the Klein-Gordon equation for a massless scalar field propagating in a spacetime whose metric is the inverse of matrix (2.23) [25]; thus, the “effective metric” (as experienced by a soundwave) would be given by

$$g_{\mu\nu}(t, \vec{x}) \equiv \frac{\rho_0}{c_s} \begin{pmatrix} -(c_s^2 - v_0^2) & \vdots & -v_0^j \\ \cdots & \cdot & \cdots \\ -v_0^i & \vdots & \delta_{ij} \end{pmatrix}. \quad (2.25)$$

If we assume that our velocity profile is strictly radial,  $\vec{v} = v_r \hat{r}$ , we may express this matrix with spherical coordinates as:

$$g_{\mu\nu} = \frac{\rho_0}{c_s} \begin{pmatrix} -(c_s^2 - v_r^2) & -v_r & 0 & 0 \\ -v_r & 1 & 0 & 0 \\ 0 & 0 & r^2 & 0 \\ 0 & 0 & 0 & r^2 \sin^2 \theta \end{pmatrix}. \quad (2.26)$$

Note that this metric does not arise from the gravitational considerations, and so it is not reasonable to expect it to satisfy any gravitational constraint.

### 2.3.2 Acoustic Horizons

Now, let us assume that our fluid in the previous section has a time-independent velocity profile that is proportional to  $1/r^{1/2}$ . For reasons that will become apparent momentarily, let us call the constant of proportionality  $\sqrt{2GM}$ . Thus, the fluid velocity will be given by:

$$\vec{v} = \sqrt{2GM/r} \hat{r}. \quad (2.27)$$

Our effective metric, equation (2.26), therefore takes the form:

$$g_{\mu\nu} = \frac{\rho_0}{c_s} \begin{pmatrix} -(c_s^2 - \frac{2GM}{r}) & -\sqrt{\frac{2GM}{r}} & 0 & 0 \\ -\sqrt{\frac{2GM}{r}} & 1 & 0 & 0 \\ 0 & 0 & r^2 & 0 \\ 0 & 0 & 0 & r^2 \sin^2 \theta \end{pmatrix}. \quad (2.28)$$

The matrix in brackets on the right hand side of this equation is recognizable as identical to the Schwarzschild metric as expressed in Painlevé-Gullstrand coordinates (only substituting the speed of light for the speed of sound, which we can set to be a constant). Please see Appendix A for a definition of the PG coordinates. It would be tempting to set the density equal to 1, and obtain an acoustic metric identical in form to the Schwarzschild black hole, however the demand that our density satisfies the continuity equation for this velocity profile imposes the constraint that:

$$\vec{\nabla} \cdot (\rho \vec{v}) = 0 \rightarrow \sqrt{2GM} \frac{\partial}{\partial r} \left( \frac{r^2 \rho_0}{r^{1/2}} \right) = 0. \quad (2.29)$$

Thus,  $\rho_0$  must go as  $r^{-\frac{3}{2}}$ .

To summarize: a flow profile with equations of state given by  $P = c_s^2 \rho$  (with  $c_s$  being constant),  $\rho_0 = \frac{\text{const.}}{r^{3/2}}$  and  $v_0 = \sqrt{\frac{2GM}{r}} \hat{r}$  gives rise to an effective acoustic metric (2.28), which is conformal to the Schwarzschild metric as expressed in PG coordinates,  $g_{\mu\nu} = K(r) g_{\mu\nu}^{PG-Schwarz}$ , where the conformal factor is  $K(r) = \frac{\rho_0}{c_s}$ .

### 2.3.3 Acoustic Hawking Radiation

Notice that acoustic metric (2.28) has a horizon precisely where we would expect in analogy to the Schwarzschild spacetime. It turns out that the existence of Hawking radiation is contingent only upon the existence of a horizon [7], and the fields in question obeying the canonical commutation relations. As we have a horizon, we should expect the emission of a thermal spectrum of soundwaves, *provided* the fluid in question is one in which sound itself is quantized (i.e, a Bose-Einstein condensate or other superfluid). This radiation will take the form of a thermal gas of phonons with a temperature given by [6]

$$T = \frac{\hbar}{2\pi k_B} \frac{\partial(v_r)}{\partial r} \quad (2.30)$$

(evaluated at the horizon), where  $k_B$  is Boltzmann's constant.

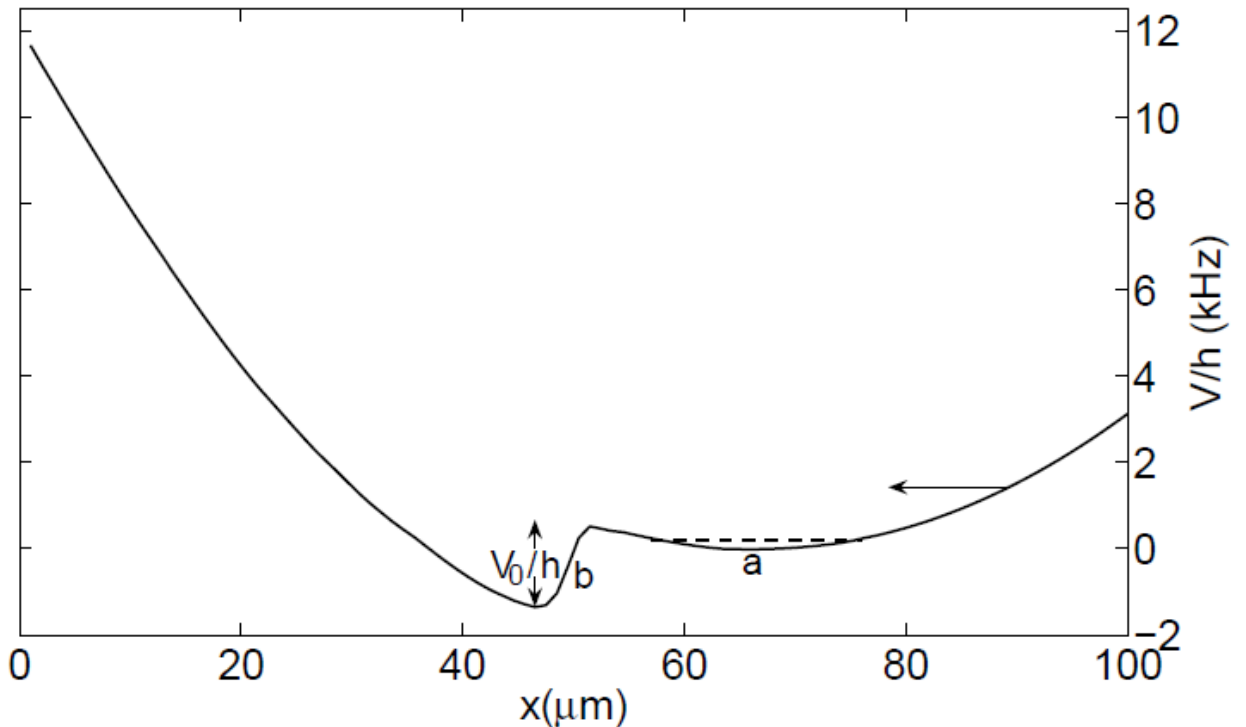


Figure 2.6: The potential experienced by the atoms of the Bose-Einstein condensate at some time before the minimum of the harmonic potential (a) is moved over to the step potential (b). The dashed line in the harmonic potential corresponds to the chemical potential of the BEC. Gravity points in the  $-x$  direction. Image taken from “Realization of a sonic black hole analogue in a Bose-Einstein condensate,” Oren Lahav et al, 2009 [2]

## 2.4 Experimental Realization

Although first proposed in 1981, the first sonic black hole was not created in the lab until 2009, by a team operating out of the Israel Institute of Technology [2].

They created a Bose-Einstein condensate consisting of approximately  $10^5$   $^{87}\text{Rb}$  atoms, each in the same state. This condensate was placed in a harmonic potential created by a magnetic trap. By adjusting the frequencies of the trap, they were able to adjust the location of the minimum of this potential along the  $x$ -axis (where they defined gravity as pointing in the negative  $x$ -direction). In this manner, they accelerated the potential until it was moving at a constant velocity of roughly 0.3mm/s in the  $-x$  direction, towards a step potential created by a half-blocked laser beam (see figure 2.6 for details).

In crossing-over the step potential, the condensate picks-up kinetic energy and is therefore accelerated. The researchers were able to gauge this change in velocity by

photographically measuring the density of the condensate before (figure 2.7 a) and after (figure 2.7 b) crossing the acoustic horizon and applying the continuity equation for particle number,  $\vec{\nabla} \cdot (n\vec{v}) = -\frac{\partial n}{\partial t}$ . In order to calculate the speed of sound in the fluid, on the other hand, the researchers made of the result  $c_s = \sqrt{gn_{ave}/m}$  for sound propagation in a Bose-Einstein condensate[26], where  $g$  is the interaction parameter,  $n_{ave}$  is the average particle density profile, and  $m$  is the atomic mass of rubidium.

In so doing, the researchers found that, after crossing over the potential, the fluid velocity is indeed greater than the speed of sound in the fluid by an order of magnitude. They were not, however, able to measure Hawking radiation, as it predicted temperature was too low to be noticeable.

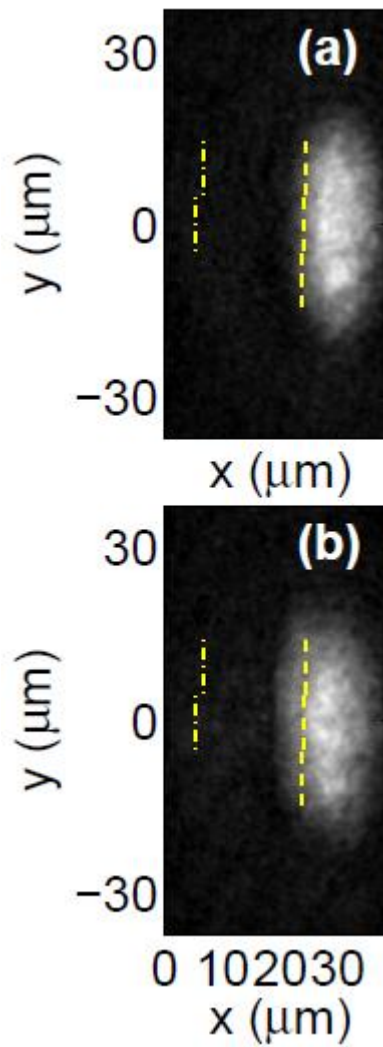


Figure 2.7: The Bose-Einstein condensate before (a) and after (b) crossing over the step potential. The dashed yellow line represents the approximate location of the acoustic horizon, while the dotted-dashed yellow line represents the position where the flow slows to a subsonic velocity. Image taken from “Realization of a sonic black hole analogue in a Bose-Einstein condensate,” Oren Lahav et al, 2009

## Chapter 3

# Derivation of the Acoustic AdS Black Hole

In the previous chapter, I explained the concept of dumb holes and demonstrated the derivation of an acoustic geometry conformal to the asymptotically flat Schwarzschild black hole. In a similar vein, I shall now provide an original derivation of an acoustic geometry conformal to the asymptotically AdS black hole, so that the quasinormal mode spectra of both acoustic black holes can be calculated in chapter 4.

### 3.1 Selecting the Proper Form of the Metric

In order to derive a fluid flow that is conformal to the Anti-de Sitter black hole spacetime it is, first of all, necessary for us to render this metric into the proper form.

Recall that, for a strictly radial fluid flow  $v_\beta \hat{\beta}$ , our “effective geometry” took the form:

$$g_{\mu\nu}^{\text{fluid}} \equiv \frac{\rho_0}{c_s} \begin{pmatrix} -(c_s^2 - v_\beta^2) & -v_\beta & 0 & 0 \\ -v_\beta & 1 & 0 & 0 \\ 0 & 0 & \beta^2 & 0 \\ 0 & 0 & 0 & \beta^2 \sin^2 \theta \end{pmatrix}, \quad (3.1)$$

Where  $\rho_0$  is the fluid mass density, and  $c_s$  is the speed of sound. Note that, for reasons that will become apparent in section 3.3, we are now going to refer to the radial coordinate of the effective metric as  $\beta$  and the temporal coordinate of the effective metric as  $\tau$ . The standard representation of the AdS-Schwarzschild geometry, by contrast, is given by:

$$g_{\mu\nu}^{\text{AdS-Schwarz:Static}} \equiv \begin{pmatrix} -(c^2 - \frac{2GM}{r} + \frac{c^2 r^2}{L^2}) & 0 & 0 & 0 \\ 0 & \frac{1}{(c^2 - \frac{2GM}{r} + \frac{c^2 r^2}{L^2})} & 0 & 0 \\ 0 & 0 & r^2 & 0 \\ 0 & 0 & 0 & r^2 \sin^2 \theta \end{pmatrix}, \quad (3.2)$$

where  $L$  is the scalar curvature of this spacetime and  $M$  is the black hole's mass.

It would be convenient if we could write this in a Painlevé-Gullstrand-like form, as we did the Schwarzschild line-element in Appendix A; and, naively, it seems like we should be able to apply the same sort of transformation, since the  $dt^2$  and  $dr^2$  terms both depend exclusively upon the radial coordinate  $r$ . However, when we actually apply this transformation (see Appendix A), we obtain the metric:

$$g_{\mu\nu}^{\text{AdS-Schwarz-PG}} = \begin{pmatrix} -(c^2 - \frac{2GM}{\beta} + \frac{\beta^2 c^2}{L^2}) & \pm \sqrt{\frac{2GM}{\beta} - \frac{\beta^2 c^2}{L^2}} & 0 & 0 \\ \pm \sqrt{\frac{2GM}{\beta} - \frac{\beta^2 c^2}{L^2}} & 1 & 0 & 0 \\ 0 & 0 & \beta^2 & 0 \\ 0 & 0 & 0 & \beta^2 \sin^2 \theta \end{pmatrix}. \quad (3.3)$$

Notice that as  $\beta$  goes to infinity, the off-diagonal terms become imaginary. As a line-element, physically, is supposed to represent the shortest distance between two points in a particular geometry, the fact that it would not be real in case should be worrisome. Moreover, comparing the metric in this form to the acoustic geometry of the conformal fluid flow, we can see that, in order to recreate this spacetime, we would need to have an *imaginary* fluid velocity. Therefore, these coordinates produce nonsensical results. If we are to find a suitable representation of the AdS-Schwarzschild metric then, we must go about it in a more subtle way.

Noting the  $\frac{\rho_0}{c_s}$  term out in front of acoustic metric (3.1), it therefore follows that, in order to be conformal to the effective geometry, a spacetime must have the general form:

$$g_{\mu\nu}^{\text{general}} = \begin{pmatrix} -f(\beta) & h(\beta) & 0 & 0 \\ h(\beta) & \Delta(\beta) & 0 & 0 \\ 0 & 0 & \Delta(\beta)\beta^2 & 0 \\ 0 & 0 & 0 & \Delta(\beta)\beta^2 \sin^2 \theta \end{pmatrix}. \quad (3.4)$$

Now, note that in general, the AdS-Schwarzschild metric in four spacetime dimensions satisfies the Einstein equations,

$$G_{\mu\nu} + \Lambda g_{\mu\nu} = 0, \quad (3.5)$$

for a value of the cosmological constant given by  $\Lambda = \frac{-3}{L^2}$ . Note also that the Schwarzschild metric in Painlevé-Gullstrand form,

$$g_{\mu\nu}^{PG} = \begin{pmatrix} -(c^2 - \frac{2GM}{\beta}) & -\sqrt{\frac{2GM}{\beta}} & 0 & 0 \\ -\sqrt{\frac{2GM}{\beta}} & 1 & 0 & 0 \\ 0 & 0 & \beta^2 & 0 \\ 0 & 0 & 0 & \beta^2 \sin^2 \theta \end{pmatrix}, \quad (3.6)$$

has flat time-slices, which makes sense since the black hole is embedded in a Minkowski spacetime. Since the black hole in our present case is embedded in an Anti-de Sitter spacetime, it seems like it would make sense to demand that our analogous representation should have time-slices given by  $AdS_3$ . This condition is satisfied if we set

$$\Delta(\beta) = \frac{4m^2 L^2}{(1 - m^2 \beta^2)^2}, \quad (3.7)$$

where  $m$  is a positive, real parameter, which, as we will see in Appendix B, can be identified with the mass of the black hole. We can now set  $G_{\mu\nu} + \Lambda g_{\mu\nu}$  equal to zero for the correct value of the cosmological constant. This yields the AdS black hole metric in the form:

$$g_{\mu\nu}^{\text{AdS-Schwarz}} = \begin{pmatrix} \frac{C_1^2(m^2\beta^2-1)}{4L^2m^2\beta} - \frac{C_2(1+m^2\beta^2)^2}{(m^2\beta^2-1)^2} & \frac{C_1}{\sqrt{\beta(m^2\beta^2-1)}} & 0 & 0 \\ \frac{C_1}{\sqrt{\beta(m^2\beta^2-1)}} & \frac{4m^2L^2}{(1-m^2\beta^2)^2} & 0 & 0 \\ 0 & 0 & \frac{4m^2L^2}{(1-m^2\beta^2)^2}\beta^2 & 0 \\ 0 & 0 & 0 & \frac{4m^2L^2}{(1-m^2\beta^2)^2}\beta^2 \sin^2 \theta \end{pmatrix}, \quad (3.8)$$

where  $C_1$  and  $C_2$  are constants to be determined. Notice that the parameter  $m$  is constrained by the off diagonal terms such that  $m^2\beta^2 \geq 1$ ; we will consider the physical implications of this constraint later in the chapter. We must now derive appropriate expressions for the parameters in the acoustic metric in order to derive

an effective geometry which is conformal to the AdS black hole.

## 3.2 Deriving the fluid parameters

We shall begin by assuming that the acoustic metric is conformal to the AdS-Schwarzschild metric (3.8): i.e, that there exists some function,  $K(\beta)$  such that  $K(\beta)$  times the AdS-Schwarzschild metric (3.8) is equivalent to the acoustic metric (3.1). We can now begin identifying the various terms, in order to derive expressions for  $\rho_0$ ,  $c_s$  and  $v_0$ , as well as the pressure  $p_0$  and the conformal factor, so that  $g_{\mu\nu}^{\text{fluid}} = K(\beta)g_{\mu\nu}^{\text{AdS-Schwarz}}$ .

By looking at the  $d\beta^2$  terms in metrics (3.1) and (3.8) , we can immediately see that

$$K(\beta)\frac{4L^2m^2}{(m^2\beta^2 - 1)^2} = \frac{\rho_0}{c_s}, \quad (3.9)$$

which implies (by looking at the off-diagonal terms) that

$$\begin{aligned} v_\beta &= -\left(\frac{c_s}{\rho_0}\right)\left(\frac{C_1}{\sqrt{\beta(\beta^2m^2-1)}}\right)K(\beta) \\ &= \frac{-C_1(m^2\beta^2-1)^{3/2}}{\sqrt{\beta}(4L^2m^2)}. \end{aligned} \quad (3.10)$$

Thus,

$$v_\beta^2 = \frac{C_1^2(m^2\beta^2 - 1)^3}{\beta(4L^2m^2)^2}, \quad (3.11)$$

so

$$\frac{\rho_0}{c_s}v_\beta^2 = \frac{C_1^2(m^2\beta^2 - 1)}{\beta(4L^2m^2)}K(\beta), \quad (3.12)$$

which agrees with the first term of  $g_{tt}^{\text{AdS-Schwarz}}$  in the gravitational metric (3.8).

By the  $dt^2$  term, then,

$$\frac{\rho_0}{c_s}c_s^2 = C_2\frac{(1 + m^2\beta^2)^2}{(m^2\beta^2 - 1)^2}K(\beta) \rightarrow c_s = \frac{\sqrt{C_2}(1 + m^2\beta^2)}{2Lm}. \quad (3.13)$$

And so,

$$\rho_0 = \frac{4L^2m^2K(\beta)}{(m^2\beta^2 - 1)^2}c_s = \frac{4L^2m^2K(\beta)\sqrt{C_2}(1 + m^2\beta^2)}{(m^2\beta^2 - 1)^2 2Lm}, \quad (3.14)$$

or, to simplify:

$$\rho_0 = \frac{\sqrt{C_2} 2Lm(1 + m^2\beta^2)K(\beta)}{(m^2\beta^2 - 1)^2}. \quad (3.15)$$

Notice that in this case,  $c_s$ , the speed of sound, is not a constant. We may find this worrisome in some ways, since the analogy between gravitational and acoustic black holes is explicitly based upon an analogy between the speed of light in a vacuum and the speed of sound in a fluid. However, if we look back at our derivation of the effective geometry experienced by sound waves (in chapter 2.3), we can notice that the assumption of a constant speed of sound never once entered into our derivation of metric (2.28). Our effective geometry therefore remains conformal to that of the AdS black hole.

### 3.2.1 Constraints from Fluid Mechanics

We now have expressions for velocity and the speed of sound, as well as a parametric expression for density. Note, however, that these quantities are constrained by the equations of fluid dynamics to behave in certain ways. In particular, the continuity equation demands that

$$\frac{\partial \rho_0}{\partial t} + \nabla \cdot (\rho_0 \vec{v}) = 0. \quad (3.16)$$

In radial coordinates, this works out to a constraint that  $\rho_0 v_\beta \sim \beta^{-2}$ . Based on identifications (3.15) and (3.10), we find that

$$\rho_0 v_\beta = \frac{-\sqrt{C_2} C_1 (1 + m^2\beta^2)}{(m^2\beta^2 - 1)^{1/2} \beta^{1/2} 2Lm} K(\beta). \quad (3.17)$$

Thus, the conformal factor can be taken as  $K(\beta) = \frac{(m^2\beta^2 - 1)^{1/2}}{(1 + m^2\beta^2)\beta^{3/2}}$ .

We can also derive an expression for the pressure, from the definition of the speed of sound:

$$\frac{dp_0}{d\rho_0} = c_s^2. \quad (3.18)$$

Multiplying both sides by  $d\rho_0$ , we obtain:

$$dp_0 = c_s^2 d\rho_0 = c_s^2 \frac{d\rho_0}{d\beta} d\beta. \quad (3.19)$$

Note, however, based on equation (3.15) and the value I just derived for  $K(\beta)$  that:

$$\rho_0 = K(\beta) \frac{\sqrt{C_2} 2Lm(1 + m^2\beta^2)}{(m^2\beta^2 - 1)^2} = \frac{\sqrt{C_2} 2Lm}{(\beta(m^2\beta^2 - 1))^{3/2}}, \quad (3.20)$$

and thus,

$$\frac{\partial \rho_0}{\partial \beta} = -\sqrt{C_2} 3Lm \frac{(3m^2\beta^2 - 1)}{(\beta(m^2\beta^2 - 1))^{5/2}}. \quad (3.21)$$

If we substitute this and our expression for  $c_s$  (equation (3.13)) into equation (3.19), we find that pressure is therefore given by:

$$\begin{aligned} p_0 &= \int c_s^2 \frac{\partial \rho_0}{\partial \beta} d\beta = \int -\frac{3C_2^{3/2}(1+m^2\beta^2)^2(3m^2\beta^2-1)}{4Lm\beta^2(m^2\beta^2-1)^2\sqrt{\beta(m^2\beta^2-1)}} d\beta \\ &= \frac{C_2^{3/2}(9m^4\beta^4-6m^2\beta^2+1)}{2\sqrt{\beta(m^2\beta^2-1)}(m^2\beta^2-1)mL\beta} \\ &= C_2^{3/2} \frac{(3m^2\beta^2-1)^2}{2Lm[\beta(m^2\beta^2-1)]^{3/2}}. \end{aligned} \quad (3.22)$$

But recall, pressure must also satisfy Euler's equation

$$\rho_0 \left( \frac{\partial \vec{v}_0}{\partial \tau} + (\vec{v}_0 \cdot \vec{\nabla}) \vec{v}_0 \right) = -\vec{\nabla} p_0. \quad (3.23)$$

At a glance, this would appear not to be satisfied by our calculated value of pressure. However, in the presence of an external force, Euler's equation gains an additional  $+\vec{f}$  term on its right-hand side:

$$\rho_0 \left( \frac{\partial \vec{v}_0}{\partial \tau} + (\vec{v}_0 \cdot \nabla) \vec{v}_0 \right) = -\nabla p_0 + \vec{f} \quad (3.24)$$

where  $\vec{f}$  is the applied force density. The force does not affect the form of the linearized Euler equation, so we are left with the same effective geometry.

Since  $v_0$  is not time-dependent, equation (3.24) gives us:

$$\frac{3(3m^6\beta^6 + 5m^4\beta^4 + m^2\beta^2 - 1)C_2^{3/2}}{4\beta^2(m^2\beta^2 - 1)^2\sqrt{\beta(m^2\beta^2 - 1)}mL} + \vec{f} = \frac{C_1^2(m^2\beta^2 - 1)^2(5m^2\beta^2 + 1)}{32\beta^2L^4m^4}, \quad (3.25)$$

from which  $\vec{f}$  can readily be discerned.

At this point, the reader may be wondering whether such an external force is also needed to “make the Euler equation work” for the flat-space conformal dumb hole with constant speed of sound derived in section (2.3). As it happens, a force term

of the form  $\vec{f}_{flat} = \left( \frac{3}{2} \frac{c_s^2}{r^{5/2}} + \frac{GM}{r^{7/2}} \right) \hat{r}$  indeed *is* required. This may cause us a moment of consternation; after all, the Anti-de Sitter black hole reduces down to a flat-space black hole in the limit of infinite radius of curvature,  $L$ ; the force term in equation (3.25), however, goes to zero as  $L \rightarrow \infty$  rather than converging towards the force term in the flat space black hole analogue.

This apparent contradiction can be resolved, however, if we note that our fluid parameters in the AdS black hole analogue (equations (3.10), (3.20), and (3.22)) also do not converge to their counterparts in the flat-space black hole analogue (summarized beneath equation (2.29)). Thus, we can regard the two dumb hole geometries as arising from two entirely different fluid flows, rather than thinking of one fluid flow as being a special case of the other.

### 3.3 Coordinate Transformation Between Metrics

We have now successfully derived a fluid metric that is conformal to the AdS Schwarzschild spacetime; it is given by metric (3.8) times the conformal factor  $K(\beta)$ , where  $K(\beta) = \frac{(m^2\beta^2-1)^{1/2}}{(1+m^2\beta^2)\beta^{3/2}}$ . However, the form of this metric is extremely inconvenient for our purposes. Not only is it rather complicated, it is not immediately obvious where the horizon or the boundary of the universe are located. We must know both in order to calculate the quasinormal modes.

Towards the goal of simplifying our calculation, let us work-out the transformation between the coordinates used in our derived metric (3.8), and the coordinates used in the standard form of the AdS-Schwarzschild spacetime (3.2). By so doing, we will be able to re-write our conformal factor,  $K(\beta)$  in terms of the coordinates used in (3.2), thereby giving us a simplified expression for the acoustic metric.

Our derived AdS-metric (3.8) is therefore now given by the expression:

$$g_{\mu\nu}^{\text{AdS-Schwarz}} = \begin{pmatrix} \frac{C_1^2(m^2\beta^2-1)}{4L^2m^2\beta} - \frac{C_2(1+m^2\beta^2)^2}{(m^2\beta^2-1)^2} & \frac{C_1}{\sqrt{\beta(m^2\beta^2-1)}} & 0 & 0 \\ \frac{C_1}{\sqrt{\beta(m^2\beta^2-1)}} & \frac{4L^2m^2}{(m^2\beta^2-1)^2} & 0 & 0 \\ 0 & 0 & \frac{4L^2m^2\beta^2}{(m^2\beta^2-1)^2} & 0 \\ 0 & 0 & 0 & \frac{4L^2m^2\beta^2 \sin^2 \theta}{(m^2\beta^2-1)^2} \end{pmatrix}. \quad (3.26)$$

We will begin by making the assumption that our transformation affects only the

radial and time coordinates. This being the case, simple identification between the angular terms in (3.2) and (3.26) allows us to say

$$r^2 = \frac{4L^2 m^2 \beta^2}{(m^2 \beta^2 - 1)^2}, \text{ or } r = \frac{2Lm\beta}{(m^2 \beta^2 - 1)}. \quad (3.27)$$

Therefore,

$$dr = \frac{-2Lm(\beta^2 m^2 + 1)}{(\beta^2 m^2 - 1)^2} d\beta, \quad (3.28)$$

or

$$dr^2 = \frac{4L^2 m^2 (\beta^2 m^2 + 1)^2}{(\beta^2 m^2 - 1)^4} d\beta^2. \quad (3.29)$$

Notice that our  $d\beta^2$  term in the metric (3.26) is given by

$$\begin{aligned} \frac{4L^2 m^2}{(m^2 \beta^2 - 1)^2} d\beta^2 &= \\ \frac{(m^2 \beta^2 - 1)^2}{(m^2 \beta^2 + 1)^2} \left( \frac{4L^2 m^2 (\beta^2 m^2 + 1)^2}{(\beta^2 m^2 - 1)^4} d\beta^2 \right) &= \frac{(m^2 \beta^2 - 1)^2}{(m^2 \beta^2 + 1)^2} dr^2. \end{aligned} \quad (3.30)$$

Likewise, the off-diagonal terms will be given by:

$$\begin{aligned} \frac{C_1}{\sqrt{\beta(-1+m^2\beta^2)}} d\beta d\tau &= \frac{C_1}{\sqrt{\beta(-1+m^2\beta^2)}} \left( \frac{-(\beta^2 m^2 - 1)^2}{2Lm(\beta^2 m^2 + 1)} \right) dr d\tau \\ &= -\frac{C_1}{2} \frac{(\beta^2 m^2 - 1)^{3/2}}{Lm\sqrt{\beta(\beta^2 m^2 + 1)}} dr d\tau. \end{aligned} \quad (3.31)$$

Using the substitution  $\beta = \frac{L + \sqrt{L^2 + r^2}}{rm}$ , we can now put the metric (3.26) in terms of the radial variable 'r,' obtaining

$$\begin{pmatrix} \frac{C_1^2}{2Lmr} - C_2 \left( 1 + \frac{r^2}{L^2} \right) & -C_1 \sqrt{\frac{L}{2m}} \frac{1}{\sqrt{r(L^2 + r^2)}} & 0 & 0 \\ -C_1 \sqrt{\frac{L}{2m}} \frac{1}{\sqrt{r(L^2 + r^2)}} & \frac{1}{1 + \frac{r^2}{L^2}} & 0 & 0 \\ 0 & 0 & r^2 & 0 \\ 0 & 0 & 0 & r^2 \sin^2 \theta \end{pmatrix}. \quad (3.32)$$

Let us now consider the constraint on  $m$  that I mentioned earlier: namely, the fact that the off-diagonal terms in metric (3.26) enforce the condition that

$$m^2 \beta^2 > 1 \quad (3.33)$$

We have now made the identification

$$\beta = \frac{L + \sqrt{L^2 + r^2}}{rm}, \quad (3.34)$$

so our constraint (3.33) in fact implies that

$$\frac{(L + \sqrt{L^2 + r^2})^2}{r^2} > 1, \quad (3.35)$$

Since  $L$  and  $r$  are each positive real numbers, this becomes

$$(L + \sqrt{L^2 + r^2})^2 > r^2,$$

$$L^2 + 2\sqrt{L^2 + r^2} + L^2 + r^2 > r^2, \quad (3.36)$$

$$L^2 + \sqrt{L^2 + r^2} > 0,$$

which is true for all legal values of  $L$  and  $r$ . Thus, it follows that  $m$  can in fact take on any positive, real value. We can now transform the standard metric (3.2) into the form of metric (3.32) by defining a time coordinate, given by:

$$\tau(t, r) = \int \left( \sqrt{1 - \frac{L^2(L + \sqrt{L^2 + r^2})^2}{(L^2 + L\sqrt{L^2 + r^2} + r^2)^2(1 - \frac{2m}{r} + \frac{r^2}{L^2})}} \right) dr + t, \quad (3.37)$$

where we have identified the black hole mass,  $M$  with the parameter  $m$  (see appendix B for details).

By comparing the results that we get from this transformation to the standard form of the metric (3.2) (with  $G = c = 1$ ), we can work out the constants in metric (3.8) to be  $C_1 = 2m\sqrt{L}$  and  $C_2 = 1$ .

We can now substitute  $\beta = \frac{L + \sqrt{L^2 + r^2}}{rm}$  into the conformal factor  $K(\beta) = \frac{(m^2\beta^2 - 1)^{1/2}}{(1 + m^2\beta^2)\beta^{3/2}}$ , thereby obtaining:

$$\begin{aligned}
\bar{K}(r) &= \frac{\sqrt{\frac{(L+\sqrt{L^2+r^2})^2}{r^2} - 1}}{\left(1 + \frac{(L+\sqrt{L^2+r^2})^2}{r^2}\right) \left(\frac{(L+\sqrt{L^2+r^2})}{mr}\right)^{3/2}} \\
&= \frac{\sqrt{2L}(L+\sqrt{L^2+r^2})^{1/2}}{\left(\frac{2r^2+2L^2+2L\sqrt{L^2+r^2}}{r}\right) \left(\frac{(L+\sqrt{L^2+r^2})}{mr}\right)} \\
&= \left(\sqrt{\frac{L}{2}}\right) \left(\frac{m^{3/2}r^{5/2}}{2r^2L+2L^3+2L^2\sqrt{L^2+r^2}+r^2\sqrt{L^2+r^2}}\right).
\end{aligned}$$

Therefore, we find that our conformal AdS dumb hole metric is given by

$$g_{\mu\nu} = \bar{K}(r) \begin{pmatrix} -(1 - \frac{2m}{r} + \frac{r^2}{L^2}) & 0 & 0 & 0 \\ 0 & \frac{1}{(1 - \frac{2m}{r} + \frac{r^2}{L^2})} & 0 & 0 \\ 0 & 0 & r^2 & 0 \\ 0 & 0 & 0 & r^2 \sin^2 \theta \end{pmatrix}, \quad (3.38)$$

where

$$\bar{K}(r) = \left(\sqrt{\frac{L}{2}}\right) \left(\frac{m^{3/2}r^{5/2}}{2r^2L + 2L^3 + 2L^2\sqrt{L^2 + r^2} + r^2\sqrt{L^2 + r^2}}\right). \quad (3.39)$$

This is the main result of chapter 3.

I have now derived a dumb hole metric which is conformal to the AdS-Schwarzschild black hole and which obeys all of the fluid equations of motion. In order to do this, it was necessary for me to derive a representation of the AdS-Schwarzschild geometry (equation (3.8)) conformal to the general fluid metric (equation (3.1)). In so doing, I was able to write expressions for the density (equation (3.15)), pressure (equation (3.22)), speed of sound (equation (3.13)), and velocity profile (equation (3.10)) of the fluid in terms of the parameters of the conformal AdS-Schwarzschild metric (that is to say  $m$ ,  $L$  and  $c = G = 1$ ). I also derived an expression for the conformal factor between the two metrics,  $K(\beta)$ , in terms of the AdS-Schwarzschild parameters. This representation of the dumb hole proved unwieldy, however, so I derived the coordinate transformations necessary to turn the representation (3.8) into the more standard representation of this geometry, (3.2). By doing so, however, I have made it rather difficult, at a glance, to tell where the fluid properties actually *are* in metric (3.38). In order to clarify this matter somewhat, I shall point-out to the reader that

the radial coordinate of metric (3.38) is in fact given by

$$r = \sqrt{\frac{\rho_0(\beta)}{c_s(\beta)K(\beta)}}\beta, \quad (3.40)$$

where  $\beta$  is the radial coordinate corresponding to the direction of fluid flow. This follows directly from comparing the angular terms in metric (3.1) to those in metric(3.38). The time coordinate of metric (3.38), meanwhile, can be expressed in terms of the fluid parameters as:

$$t = \int \frac{v_\beta}{(c_s^2 - v_\beta^2)} d\beta + \tau. \quad (3.41)$$

where  $\tau$  is the temporal coordinate in metric (3.1). If we apply these transformations to metric (3.1), we find an expression for metric 3.38 in terms of the fluid properties, namely:

$$ds^2 = \left(\frac{\rho_0}{c_s}\right) (-c_s^2 - v_\beta^2) dt^2 + \left(\frac{3v_\beta^2}{(c_s^2 - v_\beta^2)} + 1\right) \left(\frac{4\rho_0(\beta)}{c_s(\beta)K(\beta)}\right) \left(\frac{c_s^2 K^2(\beta)}{\rho_0'(\beta)c_s(\beta)K(\beta) - \rho_0(\beta)(c_s'(\beta)K(\beta) + c_s(\beta)K'(\beta))}\right)^2 dr^2 + \beta^2 d\Omega^2. \quad (3.42)$$

We can write this even more instructively if we note that equation (3.17) tells us that  $K(\beta)$  is some constant multiple of  $\frac{1}{\beta^2 \rho_0 v_\beta}$ . Thus, our metric becomes:

$$ds^2 = \left(\frac{\rho_0}{c_s}\right) (-c_s^2 - v_\beta^2) dt^2 + \left(\frac{3v_\beta^2}{(c_s^2 - v_\beta^2)} + 1\right) \left(\frac{4v_\beta(\beta)c_s^3(\beta)}{\beta\rho(\beta)c_s(\beta)v_\beta'(\beta) + v_\beta(\beta)(2\beta c_s(\beta)\rho'(\beta) + \rho(\beta)(2c_s(\beta) - \beta c_s'(\beta)))}\right) dr^2 + \beta^2 d\Omega^2, \quad (3.43)$$

from which it is possible to see directly how everything arises from fluid mechanics.

In the next chapter, we will be using metric (3.38) in order to work-out the quasinormal mode spectrum of this spacetime.

## Chapter 4

# Quasinormal Modes of Acoustic Black Holes

When discussing the quasinormal mode spectrum of an acoustic black hole, it is necessary to take into account what is and is not physically meaningful. Towards that end, let us recall the three types of quasinormal modes enumerated in chapter two: scalar, electromagnetic and gravitational.

The gravitational modes arise from perturbations of the Einstein field equations,

$$G_{\mu\nu} + \Lambda g_{\mu\nu} = 0. \quad (4.1)$$

Since the dynamics of an acoustic black hole are not governed by Einstein's field equations, clearly it is not meaningful to discuss the behaviour of their perturbations in this case.

Likewise, the electromagnetic quasinormal modes are derived from perturbations of Maxwell's equations in curved spacetimes:

$$\partial_\mu (\sqrt{-g} g^{\mu\nu} g^{\sigma\rho} F_{\nu\rho}) = 0. \quad (4.2)$$

These equations, of course, govern the behaviour of light in a particular geometry. Our acoustic geometry, however, only governs sound propagation, and is not experienced by light. Once again, therefore, we can dismiss these modes as not being physically meaningful.

It is only useful to discuss the scalar quasinormal modes; we have already demonstrated (see chapter 2, section 3) that the scalar field  $\Psi$  (defined such that  $\vec{\nabla}\Psi = \vec{v}$ )

obeys the Klein-Gordon equation,

$$\frac{1}{\sqrt{-g}} \frac{\partial}{\partial x^\mu} \left( \sqrt{-g} g^{\mu\nu} \frac{\partial}{\partial x^\nu} \Psi \right) = 0, \quad (4.3)$$

for an effective gravitational metric  $g_{\mu\nu}$ . Recall that we have identified perturbations of this scalar field with sound waves; thus, when we speak of scalar QNMs in this case, what we are in fact discussing is the behaviour of damped sonic ringing modes.

## 4.1 Quasinormal Modes of Acoustic Geometries Conformal to Asymptotically-Anti de Sitter Black Holes

Some theoretical attention has been paid to the calculation of the quasinormal mode spectra of acoustic black holes in the past [27] [28] [29] [30].

Here, I will make use of the Frobenius method, the specific application of which to AdS spacetimes is provided by Horowitz and Hubney [14]. According to this method, I will begin by writing the Klein-Gordon equation as a radial wave equation, to which I will approximate an ingoing series solution in the vicinity of the horizon. I will then bring the solution over to spatial infinity. In so doing, I will obtain a high-order polynomial in terms of  $\omega$ , which I will equate (as per the Dirichlet boundary conditions) to zero. In this fashion, I can calculate the frequency eigenvalues of the quasinormal modes.

Recall (as derived in Chapter 3) that our acoustic AdS black hole has the form

$$\begin{bmatrix} -\bar{K}(r)F(r) & 0 & 0 & 0 \\ 0 & \bar{K}(r)/F(r) & 0 & 0 \\ 0 & 0 & \bar{K}(r)r^2 & 0 \\ 0 & 0 & 0 & \bar{K}(r)r^2 \sin^2 \theta \end{bmatrix}, \quad (4.4)$$

where

$$\bar{K}(r) = \left( \sqrt{\frac{L}{2}} \right) \left( \frac{M^{3/2} r^{5/2}}{2r^2 L + 2L^3 + 2L^2 \sqrt{L^2 + r^2} + r^2 \sqrt{L^2 + r^2}} \right) \quad (4.5)$$

and

$$F(r) = \left(1 - \frac{2M}{r} + \frac{r^2}{L^2}\right). \quad (4.6)$$

As it stands right now, the boundary of the universe is at  $r = \infty$  and the event horizon is located at the point

$$r_0 = \frac{1}{3}(27ML^2 + 3\sqrt{3L^6 + 81M^2L^4})^{1/3} - \frac{L^2}{(27ML^2 + 3\sqrt{3L^6 + 81M^2L^4})^{1/3}} \quad (4.7)$$

(as calculated by solving  $F(r) = 0$  for  $r$ ).

As this is not very convenient for our purposes, let us define a new coordinate,  $x = \frac{r_0}{r}$  such that  $x \rightarrow 1$  as  $r \rightarrow r_0$  and  $x \rightarrow 0$  as  $r \rightarrow \infty$ . Now,  $r = \frac{r_0}{x} \Rightarrow dr = -\frac{r_0}{x^2}dx$ , so the metric can be rewritten as

$$\begin{bmatrix} -k(x)f(x) & 0 & 0 & 0 \\ 0 & \frac{k(x)r_0^2}{f(x)x^4} & 0 & 0 \\ 0 & 0 & k(x)\left(\frac{r_0}{x}\right)^2 & 0 \\ 0 & 0 & 0 & k(x)\left(\frac{r_0}{x}\right)^2 \sin^2 \theta \end{bmatrix}, \quad (4.8)$$

where

$$k(x) = \frac{\sqrt{2}\sqrt{L}M^{3/2}\left(\frac{r_0}{x}\right)^{5/2}}{\left(L + \sqrt{L^2 + \frac{r_0^2}{x^2}}\right)^3 + \frac{r_0^2\left(L + \sqrt{L^2 + \frac{r_0^2}{x^2}}\right)}{x^2}} \quad (4.9)$$

and

$$f(x) = 1 - \frac{2Mx}{r_0} + \frac{r_0^2}{L^2x^2}. \quad (4.10)$$

But note that

$$F(r_0) = 1 - \frac{2M}{r_0} + \frac{r_0^2}{L^2} = 0 \Rightarrow \frac{2M}{r_0} = 1 + \frac{r_0^2}{L^2},$$

so

$$\begin{aligned} f(x) &= 1 - \frac{2Mx}{r_0} + \frac{r_0^2}{L^2x^2} = 1 - x\left(1 + \frac{r_0^2}{L^2}\right) + \frac{r_0^2}{L^2x^2} \\ &= 1 - x + \frac{r_0^2}{L^2} \left(\frac{1-x^3}{x^2}\right) \\ &= 1 - x + \frac{r_0^2}{L^2} \left(\frac{(1-x)(1+x+x^2)}{x^2}\right) \\ &= (1-x) \left(1 - \frac{r_0^2(1+x+x^2)}{x^2L^2}\right) \\ f(x) &= (1-x) \left(\frac{x^2L^2 - r_0^2(1+x+x^2)}{x^2L^2}\right). \end{aligned} \quad (4.11)$$

Now consider the Klein-Gordon equation (4.3). Let us define a wave function

$$\Psi(t, x, \theta, \phi) = \psi(x)Y_{l,m}(\theta, \phi)e^{-i\omega t}, \quad (4.12)$$

where we are taking advantage of the spherical symmetry of the geometry to write the wave function as a product of a radial function  $\psi(x)$  and the Spherical Harmonics  $Y_{lm}(\theta, \phi)$  (where  $l$  and  $m$  are integers). As we are dealing with quasinormal modes, the frequency,  $\omega$  in the time-dependence term is complex.

The resulting differential equation can be separated in variables to produce the radial wave equation:

$$\left( \frac{r_0^2 \omega^2}{x^4 f(x)^2} - \frac{l(l+1)}{x^2 f(x)} \right) \psi(x) + \left( \frac{f'(x)}{f(x)} + \frac{k'(x)}{k(x)} \right) \psi'(x) + \psi''(x) = 0, \quad (4.13)$$

with  $l$ , the angular momentum quantum number, equal to  $0, 1, 2, \dots$

Let us call  $P(x) = \left( \frac{f'(x)}{f(x)} + \frac{k'(x)}{k(x)} \right)$  and  $Q(x) = \left( \frac{r_0^2 \omega^2}{x^4 f(x)^2} - \frac{l(l+1)}{x^2 f(x)} \right)$  so our d.e is

$$\psi''(x) + P(x)\psi'(x) + Q(x)\psi(x) = 0. \quad (4.14)$$

Note that the coefficients of the equation (and therefore the quasinormal frequencies) do not depend upon the quantum number  $m$ .

By looking at the definitions of  $f(x)$  and  $k(x)$ , we can see that  $P(x)$  goes as  $\frac{1}{1-x}$  and  $Q(x)$  goes as  $\frac{1}{(1-x)^2}$  near the horizon  $x = 1$ ; therefore,  $x = 1$  is a regular singular point of this differential equation. That is to say, we can construct two linearly-independent series solutions to (4.14) about the horizon using the Frobenius method (see for example [31]).

Towards this end, let us expand both  $P(x)$  and  $Q(x)$  as Taylor series about  $x = 1$ , and assume that  $\psi(x)$  has the form

$$\psi(x) = (1-x)^R \sum_{n=0}^{\infty} c_n (1-x)^n, \quad (4.15)$$

where  $R$  is a constant to be determined and the  $c_n$  are recursively defined in terms of one another, with  $n = 0, 1, 2, \dots$ . The entire differential equation is equal to zero; thus, it follows that the coefficient of each power of  $(1-x)$  must itself be equal to zero. By looking at the coefficient of  $(1-x)^{R-2}$  (the lowest exponential power), we can extract a value of  $R$ . We have  $c_0 \left( r^2 + \frac{r_0^2 \omega^2 L^4}{(L^2 + 3r_0^2)^2} \right) = 0$ , which, assuming non-trivial constants,

gives us

$$R = \pm \frac{ir_0\omega L^2}{3r_0^2 + L^2}. \quad (4.16)$$

Thus we have two linearly independent solutions, one corresponding to each value of the exponent  $R$ . One of these solutions will be “ingoing” (that is to say, moving towards  $x = 1$  as time increases) and one of them will be outgoing (that is to say that it will be moving *away* from  $x = 1$  as time increases). As our boundary conditions demand that the quasinormal modes be purely ingoing at the horizon, it is imperative that we accurately determine which is which.

In order to facilitate this determination, let us consider the case of a pair of simple plain waves of the form  $\Psi(u, t) = C_{\pm} e^{-i\omega t} e^{\pm iku}$ , where  $k$  is the wavenumber and the  $C_{\pm}$  are proportionality constants.

We may re-write this as

$$\begin{aligned} \Psi &= C_+ e^{+ik(u - \frac{\omega}{k}t)} + C_- e^{+ik(u - \frac{\omega}{k}t)} \\ &= C_+ (\cos(ku - \omega t) + i \sin(ku - \omega t)) + C_- (\cos(ku - \omega t) - i \sin(ku - \omega t)). \end{aligned} \quad (4.17)$$

Plotting the real parts of these wavefunctions (figure (4.1)), it is clear that  $C_+ e^{+ik(u - \frac{\omega}{k}t)}$  is the solution propagating in the positive  $u$ -direction, and  $C_- e^{-ik(u - \frac{\omega}{k}t)}$  is the solution propagating in the negative  $u$ -direction.

In the same fashion, we may incorporate our  $e^{-i\omega t}$  time dependence into equation (4.15), and write:

$$e^{-i\omega t} (1 - x)^{\pm \frac{ir_0 L^2 \omega}{3r_0^2 + L^2}} (\text{“Polynomial in terms of } (1 - x)\text{”}). \quad (4.18)$$

Near  $x = 1$ , we may write this as:

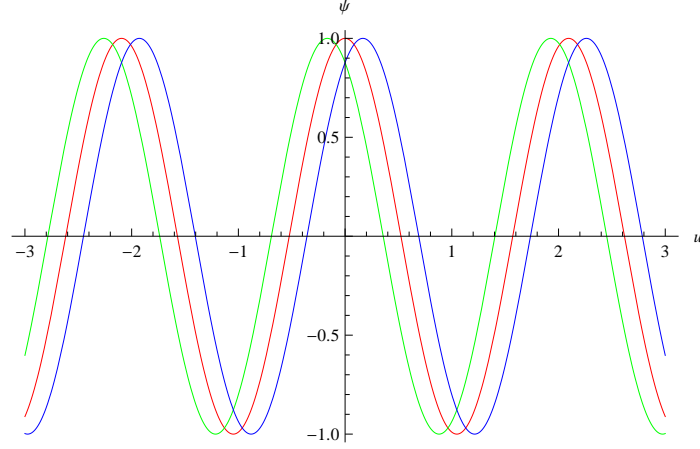


Figure 4.1: The behaviour of the real part of a simple plane wave for increasing values of  $t$ . The red (medium-shade) curve represents both ingoing and outgoing solutions (with  $C_- = C_+ = 1$ ) at  $t = 0$ . As time increases, we see that our  $C_+ e^{+ik(u - \frac{\omega}{k}t)}$  term (in green/lightest shade) moves to the left, whereas our  $C_- e^{-ik(u - \frac{\omega}{k}t)}$  (in blue/darkest shade) moves to the right.

$$\begin{aligned}
C_{\pm} e^{-i\omega t} e^{\ln(1-x) \pm \frac{ir_0\omega}{3r_0^2 L^{-2}+1}} &= C_{\pm} e^{-i\omega t \pm \frac{ir_0\omega}{3r_0^2 L^{-2}+1} \ln(1-x)} \\
&= C_{\pm} e^{\pm \frac{ir_0\omega}{3r_0^2 L^{-2}+1} (\ln(1-x) \mp \frac{3r_0^2 L^{-2}+1}{ir_0} t)} \\
&= C_{\pm} \cos\left(\frac{r_0\omega}{3r_0^2 L^{-2}+1} (\ln(1-x) \mp \frac{3r_0^2 L^{-2}+1}{ir_0} t)\right) \\
&\mp \sin\left(\frac{r_0\omega}{3r_0^2 L^{-2}+1} (\ln(1-x) \mp \frac{3r_0^2 L^{-2}+1}{ir_0} t)\right).
\end{aligned} \tag{4.19}$$

We may once again graphically observe the behaviour of these modes with increasing time (figure 4.2). Since  $\frac{r_0}{3r_0^2 L^{-2}+1}$  will be greater than zero for all physical values of the parameters, the solution corresponding to  $R = -\frac{ir_0\omega}{3r_0^2 L^{-2}+1}$  is the ingoing one, and therefore the one that we are looking for.

Now that we have a value for  $R$ , we may continue with our process of equating the coefficients of each power of  $(1-x)$  to zero. Notice that there is no condition on  $c_0$ : its value of is completely arbitrary. For the sake of the simplicity, let us set  $c_0 = 1$ . Examining the coefficient of the second-to-lowest power,  $(1-x)^{R-1}$  (and recalling that it must also be equal to zero), we can obtain a definition of  $c_1$  in terms of  $c_0 = 1$ . We can likewise define  $c_2$  in terms of  $c_1$  and  $c_0$ , and so on.

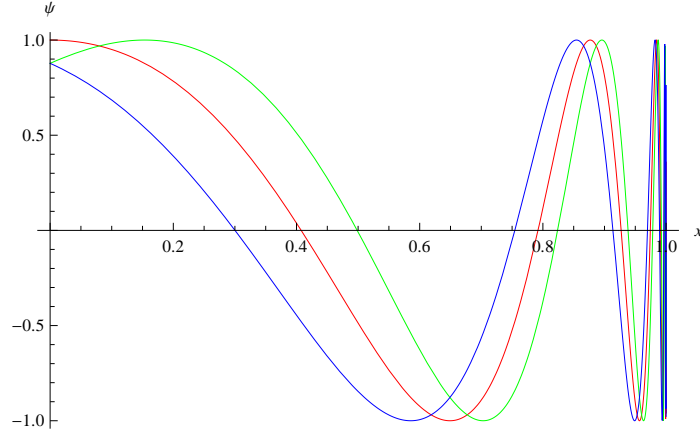


Figure 4.2: The behaviour of the real parts of our quasinormal mode solutions for increasing values of  $t$ . The red (medium-shade) curve represents both ingoing and outgoing solutions (with  $C_- = C_+ = 1$ ) at  $t = 0$ . As time increases, we see that our  $C_-$  term (in green/lightest shade) moves towards the horizon, whereas our  $C_+$  term (in blue/darkest shade) moves away from it.

Ultimately, we end up with a solution in the vicinity of the horizon of the form

$$\psi(x) = (1-x)^{-\frac{ir_0\omega}{3r_0^2L^{-2}+1}} \sum_{n=0} c_n (1-x)^n, \quad (4.20)$$

where we note that each coefficient  $c_n$  is a function of the parameters  $L, M, l$  and the frequency  $\omega$ .

Before we go about applying the vanishing boundary condition at spatial infinity (i.e, the condition that the solution go to zero, as discussed in Chapter 2, section 2), it is necessary for us to demonstrate that this condition is actually useful: that is to say, that our solution actually *can* go to zero, or, contrarily, that it does not *automatically* go to zero (in which case our imposition of boundary conditions would tell us nothing). Towards that end, let us note that in (4.13), as  $x \rightarrow 0$ ,  $P(x)$  goes as  $\frac{1}{x}$  and  $Q(x)$  goes as a constant;  $x = 0$  (which corresponds to the boundary) is therefore a regular singular point, and we can construct a pair of Frobenius solutions of differential equation (4.13) about it. In the exact same manner as when we found the solutions in the vicinity of the horizon, we find two solutions of the form:

$$\psi(x) = x^S \sum_{n=0} a_n x^n, \quad (4.21)$$

where the indices of the solution,  $S$ , are in this case given by  $S = \frac{5}{2}$  and  $S = 0$ . In

general, our ingoing solution at the horizon is going to be equivalent to some linear combination of these solutions at the boundary. Since the  $S = 0$  solution does not automatically go to zero, we can therefore conclude that our imposition of vanishing boundary conditions will actually be informative.

In order to apply the boundary condition at the edge of the universe, we bring our horizon solution, equation (4.20) over the boundary by taking the limit as  $x \rightarrow 0$  in (4.20). By so doing, we obtain

$$\psi(x \rightarrow 0) = \sum_{n=0}^{\infty} c_n(L, M, l, \omega), \quad (4.22)$$

where the  $c_n$  are the constant coefficients which depend upon  $L, M, l$  and  $\omega$ . Dirichlet boundary conditions demand that this expression must be equivalent to 0. For particular values of the parameters  $L, M$  and  $l$ , we may solve this expression numerically (for a sufficiently large value of  $n$ ) to obtain the frequency eigenvalues. The equation was solved using the computer algebra program Mathematica, and the results are summarized in Table 4.1.

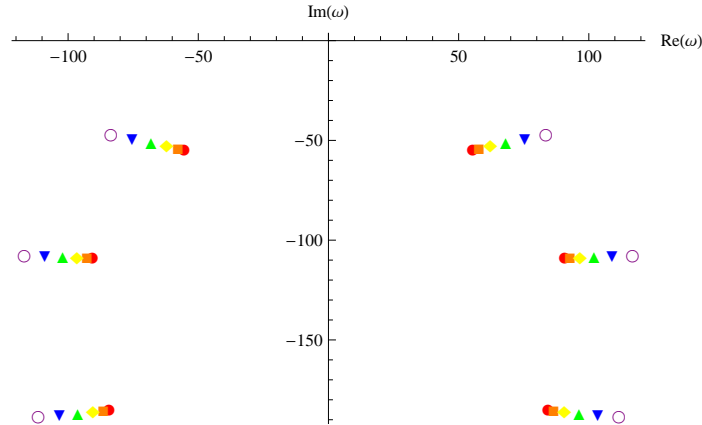


Figure 4.3: The QNM frequencies,  $M\omega$  plotted in the complex plane for various values of  $l$ , with  $\frac{M}{L} = 10$ . Red (solid circular) points correspond to  $l = 0$ , orange (square) to  $l = 1$ , yellow (diamond) to  $l = 2$ , green (upward-facing triangle) to  $l = 3$ , blue (downward-facing triangle) to  $l = 4$  and violet (hollow circle) to  $l = 5$ . The frequency scales in units of  $\text{length}^{-1}$ .

Table 4.1: Real and imaginary components of the frequency eigenvalues,  $\omega M$ , for scalar perturbations of the AdS Schwarzschild conformal dumb hole, for various values of the angular quantum number with  $\frac{M}{L} = 10$ .

<b>l</b>	<b>Re(<math>M\omega</math>)</b>	<b>Im(<math>M\omega</math>)</b>	<b>l</b>	<b>Re(<math>M\omega</math>)</b>	<b>Im(<math>M\omega</math>)</b>
<b>0</b>	-90.6981	-108.782	<b>3</b>	-102.077	-108.301
	-84.3212	-184.958		-96.2845	-186.805
	-55.4715	-54.5615		-68.1482	-51.0254
	55.4715	-54.5615		68.1482	-51.0254
	84.3212	-184.958		96.2845	-186.805
	90.6981	-108.782		102.077	-108.301
<b>1</b>	-92.7136	-108.696	<b>4</b>	-108.907	-108.041
	-86.4575	-185.335		-103.361	-187.65
	-57.8004	-53.8837		-75.3728	-49.1726
	57.8004	-53.8837		75.3728	-49.1726
	86.4575	-185.335		103.361	-187.65
	92.7136	-108.696		-108.907	-108.041
<b>2</b>	-96.5896	-108.529	<b>5</b>	-116.83	-107.783
	-90.5442	-185.995		-111.492	-188.453
	-62.1644	-52.6477		-83.5524	-47.201
	62.1644	-52.6477		83.5524	-47.201
	90.5442	-185.995		111.492	-188.453
	96.5896	-108.529		116.83	-107.783

## 4.2 Quasinormal Modes of Acoustic Geometries Conformal to Asymptotically Flat Black Holes

I am now going to turn my attention the rather incidental question of the QNM spectrum of the flat-space Schwarzschild-conformal dumb hole. Unfortunately, the Frobenius method used in the previous section cannot be brought to bear against this acoustic geometry, metric (2.28). The reason for this, ultimately, is that is not possible to construct Frobenius solutions for this geometry at asymptotic infinity: as such, the boundary condition there (which in this case is *outgoing* rather than *vanishing*) cannot be implemented by this method.

I therefore calculated the quasinormal modes of metric (2.28) using a method devised by EW Leaver in [32] and refined in [11].

To begin, let us determine the radial wave equation. We will assume that our metric has the form

$$\begin{bmatrix} -f(r) & 0 & 0 & 0 \\ 0 & g(r) & 0 & 0 \\ 0 & 0 & r^{1/2} & 0 \\ 0 & 0 & 0 & r^{1/2} \sin(\theta) \end{bmatrix}. \quad (4.23)$$

Now, using the same technique that we used in the previous section, let us define the wave function

$$\Psi(t, r, \theta, \phi) = \frac{\psi(r)}{r} Y_{lm}(\theta, \phi) e^{-i\omega t}, \quad (4.24)$$

and plug it into the Klein-Gordon equation (4.3), obtaining

$$\begin{aligned} & \left( \frac{e^{-i\omega t} Y_{lm}(\theta, \phi) \sin \theta \sqrt{rg(r)}}{r \sqrt{f(r)}} \right) \left[ \psi(r) \left( \omega^2 - \frac{l(l+1)f(r)}{\sqrt{r}} + \frac{3f(r)}{2r^2g(r)} - \frac{f'(r)}{2rg(r)} + \frac{f(r)g'(r)}{2rg(r)^2} \right) \right. \\ & \left. + \left( \frac{-3f(r)}{2rg(r)} + \frac{f'(r)}{2g(r)} - \frac{f(r)g'(r)}{2g(r)^2} \right) \psi'(r) + \frac{f(r)}{g(r)} \psi''(r) \right] = 0. \end{aligned} \quad (4.25)$$

Now, recall from equation (2.28) that the metric for the Schwarzschild-conformal

dumb hole in flat space is given by

$$g_{\mu\nu} = \frac{1}{r^{3/2}} \begin{bmatrix} -(1 - \frac{2M}{r}) & \pm\sqrt{\frac{2M}{r}} & 0 & 0 \\ \pm\sqrt{\frac{2M}{r}} & 1 & 0 & 0 \\ 0 & 0 & r^2 & 0 \\ 0 & 0 & 0 & r^2 \sin^2 \theta \end{bmatrix}. \quad (4.26)$$

Since the transformation between the standard and PG representations of the Schwarzschild spacetime is of the temporal coordinate only (see Appendix A), our conformal factor will be unaffected if we write this as a diagonal matrix

$$g_{\mu\nu} = \frac{1}{r^{3/2}} \begin{bmatrix} -(1 - \frac{2M}{r}) & 0 & 0 & 0 \\ 0 & \frac{1}{(1 - \frac{2M}{r})} & 0 & 0 \\ 0 & 0 & r^2 & 0 \\ 0 & 0 & 0 & r^2 \sin^2 \theta \end{bmatrix}. \quad (4.27)$$

By comparing metric (4.23) with metric (4.27), we can make the identifications:

$$f(r) = r^{-3/2} \left(1 - \frac{1}{r}\right) \quad (4.28)$$

and

$$g(r) = \frac{r^{-3/2}}{(1 - \frac{1}{r})} \quad (4.29)$$

(with  $2M = 1$ ).

Plugging these into equation (4.25), we obtain the differential equation

$$\begin{aligned} & \frac{(-1+r)^2}{r^2} \psi''(r) + \frac{(5-3r)(r-1)}{2r^3} \psi'(r) \\ & + \left( \frac{5+2r(-4+l(l+1))+r^2(3-2l(l+1))+2r^4\omega^2}{r^4} \right) \psi = 0. \end{aligned} \quad (4.30)$$

This second-order differential equation has regular singular points at the origin ( $r = 0$ ) and at the horizon, ( $r = 1$ ), as well as an irregular singularity as  $r \rightarrow \infty$ . We are not concerned with the interior structure of the dumb hole, so the singularity at the origin is of no particular importance to us.

Using the method of section (4.1), it can be shown that, at the horizon, the solutions behave as  $(r - 1)^{\pm i\sqrt{2}\omega}$ . As  $r$  becomes large, equation (4.25) can be solved by  $e^{\pm i\sqrt{2}\omega r}$ . If we then approximate the solution as being  $e^{-i\sqrt{2}\omega r} \Phi(r)$ , we find that

the solutions go as  $\exp(\pm i\sqrt{2}\omega(r + \ln r))$ .

For this case, we of course require the boundary conditions that the wave function be ingoing at the horizon and outgoing at spatial infinity. Using the method employed in the previous section, it can be shown that this implies that the solution must go as  $(r - 1)^{-i\sqrt{2}\omega}$  at  $r = 1$  and as  $\exp(+i\sqrt{2}\omega(r + \ln r))$  at infinity.

Let us now assume that the solution is an infinite power series of the form:

$$\psi(r) = (r - 1)^{-i\sqrt{2}\omega} r^{i2\sqrt{2}\omega} e^{i\sqrt{2}\omega(r-1)} \sum_{n=0}^{\infty} a_n \left( \frac{r-1}{r} \right)^n, \quad (4.31)$$

which, we may notice, has the correct behaviour in both limits, provided that the series converges. The requirement that the power series converges as  $r \rightarrow \infty$  is, in fact, the condition that yields the quasi-normal mode spectrum.

By plugging function (4.31) in to the differential equation, we obtain the expression:

$$\sum_{n=0}^{\infty} a_n (\alpha_n y^n + \beta_n y^{n+1} + \gamma_{n+1} y^{n+2} + \delta_{n+3} y^{n+3}) = 0, \quad (4.32)$$

with  $y = \left( \frac{r-1}{r} \right)$ , where

$$\begin{aligned} \alpha_n &= (2(n+1)^2 - 4i\sqrt{2}\omega(n+1)), \\ \beta_n &= (-4 + 20i\sqrt{2}\omega n - 7n + 32\omega^2 - 6n^2 - 4\lambda + 11i\sqrt{2}\omega), \\ \gamma_n &= (14(n-1) - 48\omega^2 + 6(n-1)^2 + 4\lambda + 14 - 24i\sqrt{2}\omega(n-1) - 28i\sqrt{2}\omega) \\ \text{and } \delta_n &= (16\omega^2 - 2(n-2)^2 + 14i\sqrt{2}\omega - 7(n-2) + 8i\sqrt{2}\omega(n-2) - 10), \end{aligned} \quad (4.33)$$

where  $\lambda = l(l+1)$ .

We can expand this as

$$\begin{aligned} &(a_0\alpha_{-1}) + (a_1\alpha_0 + a_0\beta_0)y + (a_2\alpha_1 + a_1\beta_1 + a_0\gamma_1)y^2 \\ &+ \sum_{n=3}^{\infty} (a_n\alpha_{n-1} + a_{n-1}\beta_{n-1} + a_{n-2}\gamma_{n-1} + a_{n-3}\delta_{n-1})y^n, \end{aligned} \quad (4.34)$$

from which we may derive a four-term recurrence relation (bearing in mind that  $\alpha_{-1} = 0$ ), given by



three-term recurrence relation

$$\alpha'_n a_{n+1} + \beta'_n a_n + \gamma'_n a_{n-1} = 0 \quad (4.39)$$

can be written as an infinite continued fraction of the form:

$$\frac{a_{n+1}}{a_n} = \frac{-\gamma'_{n+1}}{\beta'_{n+1}-} \frac{\alpha'_{n+1}\gamma'_{n+2}}{\beta'_{n+2}-} \frac{\alpha'_{n+2}\gamma'_{n+3}}{\beta'_{n+3}-} \dots, \quad (4.40)$$

which will converge to a constant in the limit of infinite  $n$  if and only if there exists some non-trivial, minimal solution sequence,  $a_n = f_n$  (where “minimal” is here defined in the sense that if there exists any other non-trivial solution sequence  $y_n$ ,  $\frac{f_i}{y_i} < 1$  for all  $i$ ) [33].

It turns out that the frequencies at which such a minimal solution sequence are defined are the same as those frequencies at which the determinant of the  $N \times N$  matrix (known as a Hill Determinant) go to zero in the limit  $N \rightarrow \infty$ . In order to calculate these values to arbitrary precision, Leaver presents the following four-step algorithm [11]:

To find the frequencies for a given  $l$ ... (i) choose an  $N$ , (ii) define a function returning the determinant of the system, (iii) find the roots of interest of this function and (iv) increase  $N$  until these roots become constant to within the desired precision.

Doing this, I obtain a spectrum of eigenfrequencies which are stable up to six significant figures for  $N$  as large as 30, summarized in table 4.2.

The question now arises as to whether or not these values of  $\omega$  constitute quasi-normal frequencies of the dumb hole. Recall, my argument is that, at this frequency eigenvalue, it is possible to define a non-trivial solution sequence  $a_n = f_n$  such that  $\lim_{n \rightarrow \infty} \frac{a_{n+1}}{a_n} = c$ , where  $c$  is a constant. By the comparison test, however,  $\sum_{n=0} f_n$  converges if  $|c| < 1$ ; that is to say that our solution series,  $\sum_{n=0} a_n \left(\frac{r-1}{r}\right)^n$ , will converge at spatial infinity (which is, of course, necessary for our boundary condition to hold).

In [11], Leaver proves that, if the series converges for the frequency eigenvalue, then the recursion coefficients must asymptotically go as

$$\alpha'_n \propto k(n^2 + un), \beta'_n \propto -k(2n^2 + vn) \text{ and } \gamma'_n \propto k(n^2 + wn), \quad (4.41)$$

Table 4.2: Real and imaginary frequency eigenvalues,  $\omega 2M$  for scalar perturbations of the flat-space Schwarzschild-conformal dumb hole, for various values of the angular quantum number.

<b>l</b>	<b>Re(<math>\omega</math>)</b>	<b>Im(<math>\omega</math>)</b>	<b>l</b>	<b>Re(<math>\omega</math>)</b>	<b>Im(<math>\omega</math>)</b>
<b>0</b>	0	-0.55644	<b>2</b>	0	- 1.18764
	0	-1.43000		0	- 1.84000
				$\pm 1.93762$	-0.99503
				$\pm 1.53195$	-0.72469
				$\pm 1.15832$	-0.45163
				$\pm 0.84841$	-0.19128
			$\pm 0.61543$	-0.05770	
<b>1</b>	0	- 0.84899	<b>3</b>	0	-1.53141
	0	- 1.5867		0	- 2.14300
	$\pm 1.85163$	- 1.04929		$\pm 2.06243$	-0.93013
	$\pm 1.41943$	- 0.78791		$\pm 1.68745$	-0.65813
	$\pm 1.00315$	-0.51955		$\pm 1.35181$	-0.39309
	$\pm 0.63501$	-0.24254		$\pm 1.07984$	-0.15615
	$\pm 0.37711$	-0.05678		$\pm 0.85401$	-0.06151

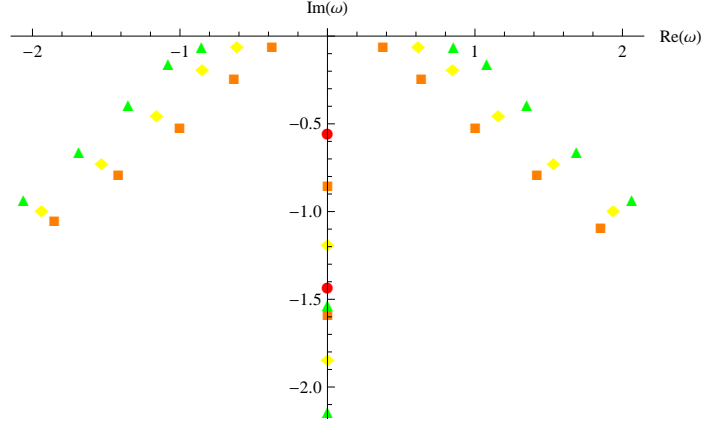


Figure 4.4: Possible spectrum of quasinormal frequencies for the Flat-Space Schwarzschild-conformal dumb hole, at varying values of the angular momentum quantum number  $l$ , with  $2M = 1$ . Red (solid circle) corresponds to  $l = 0$ , orange (square) to  $l = 1$ , yellow (diamond) to  $l = 2$  and green (upward-facing triangle) to  $l = 3$ . The frequency scales in units of  $\text{length}^{-1}$ .

where  $k, u, v$  and  $w$  are constants. Moreover,

$$\frac{a_{n+1}}{a_n} \approx 1 + \frac{a}{\sqrt{n}} + \frac{b}{n} + \dots, \quad (4.42)$$

with  $a^2 = u - v - w$  and  $b = \frac{1}{4} + \frac{v}{2} - u$ .

Let us now attempt to derive the constants  $u, v, w$  and  $k$ . In the limit of large  $n$ ,  $\alpha'_n$  goes as  $2n^2 + (4 - 4i\sqrt{2}\omega)n$ . Thus,  $k = 2$  and  $u = 2 - 2i\sqrt{2}\omega$ . Recall that  $\beta'_n = \beta_n - \alpha'_{n-1} \frac{\delta_n}{\gamma'_{n-1}}$ . From the definition of  $\alpha'_n$  we find that  $\alpha'_{n-1} \approx 2(n^2 - 2i\sqrt{2}\omega)$ .  $\beta_n$  and  $\delta_n$  meanwhile, go as  $-6n^2 - (7 - 20i\sqrt{2}\omega)n$  and  $-2n^2 + (1 + 8i\sqrt{2}\omega)n$ , respectively.

We assume that  $\gamma'_n$  goes as  $2(n^2 - wn)$ , and therefore obtain the expression  $\beta'_n \approx -2(2n^2 + (-4i\sqrt{2}\omega + 2 + w)n)$ , from which we see that  $v = -4i\sqrt{2}\omega + 2 + w$ . Similarly, we can find that  $\gamma'_n$  goes as  $2(1 + w)$ . Note, however, that this last expression does not specify a value for  $w$  beyond the trivial tautology,  $w = w$ . Plugging these expressions into 4.42, we find that we have

$$\frac{a_{n+1}}{a_n} \approx 1 \pm \frac{\sqrt{-2i\sqrt{2}\omega}}{\sqrt{n}} + \frac{1}{n} \left( \frac{w}{2} - \frac{3}{4} \right). \quad (4.43)$$

Clearly, we are not able to obtain a specific value for  $b$ . Thus, it remains unclear whether or not our solution actually converges at infinity. Thus, the most that we can conclude about the quasinormal mode spectrum of this acoustic black hole is that

if such modes exist, they must have frequency values specified in table (4.2). The problem of whether or not the wave function is actually defined at infinity remains unsolved.

I have now derived both the quasinormal spectrum of the dumb-hole conformal to the asymptotically AdS black hole, and a possible quasinormal spectrum for the Dumb Hole conformal to the asymptotically flat black hole. Due to the nature of the AdS-Schwarzschild conformal geometry, and the vanishing condition at infinity, the calculation of the first set of frequencies was done fairly straightforwardly using the Frobenius method. The flat space Schwarzschild-conformal geometry, by contrast, proved much less amenable to analysis. While a possible quasinormal frequency spectrum was derived using the method of E. Leaver, it remains unknown whether the solution is in fact defined at spatial infinity.

# Chapter 5

## Conclusions

I have successfully computed the quasinormal mode spectrum of an acoustic Anti-de Sitter black hole analogue for specified values of its parameters using the Frobenius method (Section 4.1). In order to do this, it was first necessary for me to *derive* this analogue (Section 3.1). I did this by means of solving the Einstein equations for an *AdS* spacetime in such a way that the resulting metric (3.8) had the same form as the effective metric experienced by soundwaves in an inviscid, irrotational and barotropic fluid flow. Through identification between the metrics, I was able to derive the correct forms of the fluid velocity, density and pressure (as well as the behaviour of the speed of sound in the fluid) necessary to produce a fluid metric conformal to my derived form of the AdS geometry (Section 3.2). By considering the limitations imposed by the fluid equations of motion, I was also able to derive an expression for the conformal factor between the two metrics.

Incidentally, I also calculated a possible quasinormal mode spectrum of the flat-space Schwarzschild conformal dumb hole, devised by Matt Visser in [23] (Section 4.2). I did this using the method of E. Leaver ([32][11]). It remains unclear, however, whether the wave function in this case is in fact defined at spatial infinity; as such, it cannot be definitively said whether this spectrum in fact represents the dumb hole's quasinormal modes.

My interest in the Anti- de Sitter black hole was motivated by the AdS-CFT correspondence, which holds that the physics of such a system in  $n$  dimensions should be equivalent to that of a quantum field theory in  $n - 1$  flat dimensions. According to this conjecture, quasinormal modes of fields in the AdS spacetime map to poles of correlation functions in the dual field theory. While I should point-out that, since our acoustic metric did not arise from gravitational considerations, it does not come

with a dual field theory, I have, however, provided an important means of simulating an AdS-Schwarzschild geometry.

# Bibliography

- [1] D. Mateos, *String Theory and Quantum Chromodynamics*, *Class.Quant.Grav.* **24** (2007) S713–S740, [[hep-th/0709.1523](#)].
- [2] O. Lahav, A. Itah, A. Blumkin, C. Gordon, S. Rinott, A. Zayats, and J. Steinhauer, *Realization of a Sonic Black Hole Analog in a Bose-Einstein Condensate*, *Physical Review Letters* **105** (Dec., 2010) 240401, [[cond-mat.quant-gas/0906.1337](#)].
- [3] S. Hawking, *Black hole explosions?*, *Nature* **248** (1974) 30–31.
- [4] S. W. Hawking, *Particle creation by black holes*, *Communications in Mathematical Physics* **43** (Aug., 1975) 199–220.
- [5] J. M. Maldacena, *The Large  $N$  limit of superconformal field theories and supergravity*, *Adv.Theor.Math.Phys.* **2** (1998) 231–252, [[hep-th/9711200](#)].
- [6] W. Unruh, *Experimental black hole evaporation*, *Phys.Rev.Lett.* **46** (1981) 1351–1353.
- [7] M. Visser, *Essential and inessential features of Hawking radiation*, *Int.J.Mod.Phys.* **D12** (2003) 649–661, [[hep-th/0106111](#)].
- [8] C. Barceló, S. Liberati, and M. Visser, *Analogue Gravity*, *Living Reviews in Relativity* **8** (Dec., 2005) 12, [[gr-qc/0505065](#)].
- [9] R. Konoplya and A. Zhidenko, *Quasinormal modes of black holes: From astrophysics to string theory*, *Rev.Mod.Phys.* **83** (2011) 793–836, [[gr-qc/1102.4014](#)].
- [10] D. T. Son and A. O. Starinets, *Minkowski space correlators in AdS / CFT correspondence: Recipe and applications*, *JHEP* **0209** (2002) 042, [[hep-th/0205051](#)].

- [11] E. W. Leaver, *Quasinormal modes of reissner-nordström black holes*, *Phys. Rev. D* **41** (May, 1990) 2986–2997.
- [12] K. D. Kokkotas and B. Schmidt, *Quasi-normal modes of stars and black holes*, *Living Reviews in Relativity* **2** (1999), no. 2.
- [13] E. Berti, V. Cardoso, and A. O. Starinets, *Quasinormal modes of black holes and black branes*, *Class.Quant.Grav.* **26** (2009) 163001, [[arXiv:0905.2975](#)].
- [14] G. T. Horowitz and V. E. Hubeny, *Quasinormal modes of AdS black holes and the approach to thermal equilibrium*, *Physics Review D* **62** (July, 2000) 024027, [[hep-th/9909056](#)].
- [15] Y. Chouquet-Bruhat, *General Relativity and the Einstein Equations*. Oxford University Press, Oxford, 2009.
- [16] S. W. Hawking and D. N. Page, *Thermodynamics of black holes in anti-de Sitter space*, *Communications in Mathematical Physics* **87** (Dec., 1982) 577–588.
- [17] E. Witten, *Anti-de Sitter space and holography*, *Adv.Theor.Math.Phys.* **2** (1998) 253–291, [[hep-th/9802150](#)].
- [18] G. 't Hooft, *A planar diagram theory for strong interactions*, *Nuclear Physics B* **72** (Apr., 1974) 461–473.
- [19] O. Aharony, S. S. Gubser, J. M. Maldacena, H. Ooguri, and Y. Oz, *Large N field theories, string theory and gravity*, *Phys.Rept.* **323** (2000) 183–386, [[hep-th/9905111](#)].
- [20] S. S. Gubser, *The little book of string theory*. Princeton University Press, Princeton, 2010.
- [21] B. Zwiebach, *A First Course in String Theory, Second Edition*. Cambridge Univ. Press, Cambridge, 2009.
- [22] P. K. Kovtun and A. O. Starinets, *Quasinormal modes and holography*, *Phys.Rev.* (2005) 086009, [[hep-th/0506184](#)].
- [23] M. Visser, *Acoustic black holes: Horizons, ergospheres, and Hawking radiation*, *Class.Quant.Grav.* **15** (1998) 1767–1791, [[gr-qc/9712010](#)].

- [24] I. Currie, *Fundamental Mechanics of Fluids, Second Edition*. McGraw-Hill Inc., Toronto, 1993.
- [25] J. A. Peacock, *Cosmological Physics*. Cambridge University Press, Cambridge, 1999.
- [26] E. Zaremba, *Sound propagation in a cylindrical bose-condensed gas*, *Phys. Rev. A* **57** (Jan, 1998) 518–521, [[cond-mat/9708237](#)].
- [27] E. Abdalla, R. Konoplya, and A. Zhidenko, *Perturbations of Schwarzschild black holes in laboratories*, *Class.Quant.Grav.* **24** (2007) 5901–5910, [[hep-th/0706.2489](#)].
- [28] S. Okuzumi and M.-a. Sakagami, *Quasinormal ringing of acoustic black holes in Laval nozzles: Numerical simulations*, *Phys.Rev.* **D76** (2007) 084027, [[gr-qc/0703070](#)].
- [29] J. Saavedra, *Quasinormal modes of Unruh’s acoustic black hole*, *Mod.Phys.Lett.* **A21** (2006) 1601–1608, [[gr-qc/0508040](#)].
- [30] E. Berti, V. Cardoso, and J. P. Lemos, *Quasinormal modes and classical wave propagation in analogue black holes*, *Phys.Rev.* **D70** (2004) 124006, [[gr-qc/0408099](#)].
- [31] D. Zill, *A First Course in Differential Equations, Eighth Edition*. Brooks/Cole, Belmont, CA, 2005.
- [32] E. Leaver, *An Analytic representation for the quasi normal modes of Kerr black holes*, *Proc.Roy.Soc.Lond.* **A402** (1985) 285–298.
- [33] W. Gautschi, *Computational aspects of three-term recurrence relations*, *SIAM Review* **9** (January, 1967) 24–82.

# Appendix A

## Derivation of Painlevé -Gullstrand-like coordinates

Suppose that we have a line-element of the form

$$ds^2 = -F(r)d\tau^2 + G(r)dr^2 + H(r)d\Omega^2 \quad (\text{A.1})$$

where  $F(r)$ ,  $G(r)$  and  $H(r)$  are continuous on the interval  $r_+$  to infinity, where  $r_+$  is the location of the apparent horizon.

Let us define a timelike coordinate  $\tau(t, r)$  such that

$$d\tau = \frac{\partial\tau}{\partial t}dt + \frac{\partial\tau}{\partial r}dr \quad (\text{A.2})$$

Thus,

$$dt = \frac{d\tau - \partial_r\tau dr}{\partial_t\tau} \Rightarrow dt^2 = \frac{d\tau^2 - 2(\partial_r\tau)drd\tau + (\partial_r\tau)^2dr^2}{(\partial_t\tau)^2} \quad (\text{A.3})$$

Substituting, we find that

$$ds^2 = \frac{-F(r)}{(\partial_t\tau)^2}d\tau^2 - \frac{2F(r)(\partial_r\tau)}{(\partial_t\tau)^2}d\tau dr + \left( \frac{-F(r)(\partial_r\tau)^2}{(\partial_t\tau)^2} + G(r) \right) dr^2 + H(r)d\Omega^2 \quad (\text{A.4})$$

We demand that the coefficient of  $dr^2$  be equal to one: that is

$$\frac{-F(r)(\partial_r\tau)^2}{(\partial_t\tau)^2} + G(r) = 1. \text{ Multiplying through, this gives us:}$$

$$-F(r)(\partial_r\tau)^2 + G(r)(\partial_t\tau)^2 = (\partial_t\tau)^2 \Rightarrow F(r)(\partial_r\tau)^2 = (G(r) - 1)(\partial_t\tau)^2,$$

$$\sqrt{F(r)}(\partial_r \tau) = \sqrt{G(r) - 1}(\partial_t \tau)$$

$$\frac{\partial \tau(r, t)}{\partial r} = \sqrt{\frac{G(r) - 1}{F(r)}} \frac{\partial \tau(r, t)}{\partial t}. \quad (\text{A.5})$$

We can solve this differential equation to find

$$\tau(t, r) = \int \left( \sqrt{\frac{G(r) - 1}{F(r)}} \right) dr + t, \quad (\text{A.6})$$

thus allowing us to derive a "Painlevé-Gullstrand-like" form of any spherically symmetric metric, by substituting appropriate values of  $F(r)$ ,  $G(r)$  and  $H(r)$  into the line-element

$$ds^2 = -F(r)d\tau^2 - 2\sqrt{F(r)(G(r) - 1)}drd\tau + dr^2 - H(r)d\Omega^2. \quad (\text{A.7})$$

In the case of the Schwarzschild black hole, for example, the relevant equations (which can be drawn from the normal representation of the line element) are

$$F(r) = 1 - \frac{2m}{r}, \quad (\text{A.8})$$

$$G(r) = \frac{1}{1 - \frac{2m}{r}} \quad (\text{A.9})$$

and

$$H(r) = r^2 \quad (\text{A.10})$$

Substituting these into metric A.7, we obtain the standard PG line element:

$$ds^2 = -\left(1 - \frac{2m}{r}\right)d\tau^2 - 2\sqrt{\frac{2m}{r}}d\tau dr + dr^2 + r^2d\Omega^2 \quad (\text{A.11})$$

## Appendix B

# Derivation of the Coordinate transformation between representations of Anti-de Sitter Black Hole Geometry

I have already shown by simple identification (section 3.3) that the radial coordinate  $r$  in the usual, static representation of the AdS black hole can be written in terms of the coordinate  $\beta$  in our derived metric (3.26) as:

$$r = \frac{2Lm\beta}{(m^2\beta^2 - 1)}. \quad (\text{B.1})$$

We are now going to work out an expression for the static time coordinate,  $t$  in terms of the derived-metric time coordinate  $\tau$  and the radial coordinate  $r$ , Subsequently, this will allow us to identify the constants in metric (3.24),  $C_1$  and  $C_2$ .

Suppose we have a line-element of the form

$$ds^2 = -f(r)dt^2 + g(r)dr^2 + r^2d\Omega^2. \quad (\text{B.2})$$

Let us define some time-like variable  $\tau(t, r)$  such that our line-element will have the form

$$ds^2 = -F(r)d\tau^2 - 2G(r)d\tau dr + H(r)dr^2 + r^2d\Omega^2 \quad (\text{B.3})$$

(that is to say, the form of our derived metric (3.32).

As we showed in Appendix A, for such a time coordinate,

$$dt^2 = \frac{d\tau^2 - 2\partial_r\tau drd\tau + (\partial_r\tau)^2 dr^2}{(\partial_t\tau)^2}, \quad (\text{B.4})$$

so we have

$$ds^2 = -\frac{f(r)}{(\partial_t\tau)^2} d\tau^2 + 2f(r)\frac{(\partial_r\tau)}{(\partial_t\tau)^2} drd\tau + \left(g(r) - f(r)\frac{(\partial_r\tau)^2}{(\partial_t\tau)^2}\right) dr^2 + r^2 d\Omega^2. \quad (\text{B.5})$$

We demand that

$$\left(g(r) - f(r)\frac{(\partial_r\tau)^2}{(\partial_t\tau)^2}\right) = H(r), \quad (\text{B.6})$$

where  $H(r)$  is the coefficient of  $dr^2$  in equation C.3.

This gives us

$$(\partial_r\tau) = \left(\sqrt{\frac{g(r) - H(r)}{f(r)}}\right) (\partial_r\tau). \quad (\text{B.7})$$

Thus

$$\tau(t, r) = \int \left(\frac{g(r) - H(r)}{f(r)}\right) dr + t. \quad (\text{B.8})$$

In our present case,

$$f(r) = \left(1 - \frac{2M}{r} + \frac{r^2}{L^2}\right), g(r) = \frac{1}{\left(1 - \frac{2M}{r} + \frac{r^2}{L^2}\right)}, \text{ and } H(r) = \frac{L^2(L + \sqrt{L^2 + r^2})^2}{(L^2 + L\sqrt{L^2 + r^2} + r^2)^2}, \quad (\text{B.9})$$

so we have

$$\tau(t, r) = \int \left(\sqrt{1 - \frac{L^2(L + \sqrt{L^2 + r^2})^2}{(L^2 + L\sqrt{L^2 + r^2} + r^2)^2(1 - \frac{2m}{r} + \frac{r^2}{L^2})}}\right) dr + t, \quad (\text{B.10})$$

so

$$(\partial_t\tau) = 1, (\partial_r\tau) = \left(\sqrt{1 - \frac{L^2(L + \sqrt{L^2 + r^2})^2}{(L^2 + L\sqrt{L^2 + r^2} + r^2)^2(1 - \frac{2m}{r} + \frac{r^2}{L^2})}}\right) \quad (\text{B.11})$$

Thus we can see that the coefficient of  $d\tau^2$  (that is  $\left(\frac{C_1^2(m^2\beta^2-1)}{4L^2m^2\beta} - \frac{C_2(1+m^2\beta^2)^2}{(m^2\beta^2-1)^2}\right)$ )

in metric 3.20) must be simply equal to  $f(r)$ . We can use this to determine the constants,  $C_1$  and  $C_2$ . To see this, let us write  $f(r) = (1 - \frac{2M}{r} + \frac{r^2}{L^2})$  as a function in terms of the derived-metric radial coordinate,  $\beta$ . By equation (B.1), we can write

$$\bar{f}(\beta) = -1 + \frac{M^2\beta^2 - 1}{L\beta} - \frac{4M^2\beta^2}{(M^2\beta^2 - 1)^2}, \quad (\text{B.12})$$

which can be straightforwardly rewritten as

$$\frac{(M^2\beta^2 - 1)}{L\beta} - \frac{(M^2\beta^2 - 1)^2 + 4M^2\beta^2}{(M^2\beta^2 - 1)^2}. \quad (\text{B.13})$$

Let us now simply identify the positive, real parameter  $m$  with the black hole's mass  $M$ ; this is a completely allowed identification, as shown in equations (3.33) through (3.36)). Thus, by simple comparison between function (B.13) and the function  $\left(\frac{C_1^2(m^2\beta^2-1)}{4L^2m^2\beta} - \frac{C_2(1+m^2\beta^2)^2}{(m^2\beta^2-1)^2}\right)$ , we can plainly see that  $C_1^2 = 4Lm^2$ , or

$$C_1 = 2m\sqrt{L} \text{ and } C_2 = 1 \quad (\text{B.14})$$